eLife

Reviewed Preprint
v1 • February 3, 2026
Not revised

For correspondence:
ssumanas@usf.edu

* Equal contribution

Competing interests: No competing interests declared

Funding: See page 23

Reviewing editor: Owen J Tamplin, University of Wisconsin-Madison, United States

Jam2 Signaling Functions Downstream of Hand2 To Initiate The Formation Of Organ-Specific Vascular Progenitors In Zebrafish

Martyna Griciunaite*, Julius Martinkus*, Sanjeeva Metikala*, Ricardo DeMoya, Suman Gurung, Diandra Rufin Florat, Saulius Sumanas

Department of Pathology and Cell Biology University of South Florida, Tampa, United States

eLife Assessment

This **important** study addresses the question of how organ-specific blood vessels form during different stages of development, and how specific genes may regulate these processes. New genetic tools were developed to label distinct endothelial cell populations and track them over time in different mutant backgrounds. The results are **solid**; however, additional data quantification, lineage tracing, and cell autonomy experiments would further strengthen the conclusions.

https://doi.org/10.7554/eLife.109406.1.sa3

Abstract

The mechanisms regulating the formation of organ-specific vasculature are still poorly understood. We have previously identified a population of late-forming endothelial progenitor cells in zebrafish embryos (termed secondary vascular field, SVF), which emerge from the lateral plate mesoderm after 24 hpf stage, after blood circulation has been initiated. Here we investigate the functional role of SVF cells and the molecular mechanisms that govern the emergence of these SVF cells and their contribution to vasculature. We identified that the bHLH transcription factor Hand2 and Junctional Adhesion Molecule Jam2b are expressed in the SVF-forming region and are required for the emergence of SVF cells in zebrafish embryos. Time-lapse imaging and *jam2b:Cre* based lineage tracing showed that SVF cells serve as the major source of the intestinal vasculature, including the supraintestinal artery (SIA) and subintestinal vein (SIV), which are subsequently remodeled to provide the blood flow to many internal organs. To analyze the functional role of *jam2b* and a related *jam2a* gene in vascular development, we generated double maternal-zygotic *jam2a; jam2b* mutants, which display a greatly reduced number of SVF cells and show defects in the intestinal vasculature development. Further analysis showed that *hand2* functions in the SVF-forming region upstream of *jam2b* and is required to induce expression of transcription factor *etv2/etsrp*, a known master regulator of vasculogenesis. In summary, our results identify new roles for Jam2 signaling and Hand2 function in the emergence of organ-specific vascular progenitors. The presence of similar progenitors in mammalian embryos suggests that this mechanism is evolutionarily conserved.

Introduction

It has been well established that organ-specific blood vessels exhibit a large diversity of specialized endothelial cells. However, their developmental origin has been debatable. Previous studies have suggested that the progenitors of internal organ vasculature in mammalian embryos form by differentiation *de novo,* or vasculogenesis.[1–4] Different studies have demonstrated that the endocardium, and endoderm or mesothelium may contribute to the organ vasculature in

mammals and avian embryos.[5–7] In contrast, several studies have argued that the posterior cardinal vein (PCV) serves as the major source of organ-specific vascular endothelial cells in zebrafish embryos.[8–10] According to this model, individual cells from the PCV migrate at 30-48 hours post fertilization (hpf) and coalesce into the intestinal vessels, which include the supraintestinal artery (SIA) and the subintestinal vein (SIV). These vessels subsequently undergo remodeling and ultimately provide blood supply for the internal organs, including the pancreas and the liver.[10] However, this model in zebrafish contrasts with the *de novo* vasculogenesis model, suggested in mammalian embryos. In addition, it is unclear if the PCV is the only or even the main source of internal organ-specific vascular progenitors.

In zebrafish, similar to mammalian embryos, the earliest vascular progenitors originate from the lateral plate mesoderm (LPM) during late gastrulation and somitogenesis, and coalesce into the major axial vessels, the dorsal aorta (DA) and the PCV.[11–14] This process is thought to be largely complete by the 24 hpf stage, when blood circulation is first initiated. We have recently demonstrated that between 24 and 48 hpf a separate group of late-forming vascular progenitors emerges from the LPM along the yolk extension at the site termed the secondary vascular field (SVF).[15] SVF cells can uniquely incorporate into the PCV after blood circulation has already been established, and show high expression of vascular progenitor markers, including *etv2/etsrp, tal1/scl, npas4l,* while they are negative for the expression of more differentiated endothelial markers such as *kdrl* or *fli1a.* Previous time-lapse imaging using *etv2* reporter lines demonstrated that SVF cells can contribute to the intestinal vasculature, including the SIA and SIV.[15] However, the ultimate fate of SVF cells has not been clear due to the absence of genetic tools to perform the lineage tracing. Furthermore, mechanisms regulating the emergence of SVF cells and their contribution to vasculature remain largely unknown.

To identify the molecular signature of SVF cells, we have previously performed transcriptomic analysis of the zebrafish trunk region at 30 hpf.[16] This analysis identified some SVF marker genes, which have not been previously associated with vascular development, including *junctional adhesion molecule 2b (jam2b).*[15] Vertebrate JAM homologs have been implicated in diverse processes including leukocyte-endothelial interaction and transendothelial migration, maintenance of hematopoietic stem cells (HSCs), vascular development, and others.[17,18] A related zebrafish paralog *jam2a* has been previously implicated in HSC formation.[19] However, the role of *jam2b* in vascular development has not been described.

Here we analyzed the role of zebrafish *jam2b* in the formation of intestinal vasculature and the emergence of SVF cells. We demonstrate that *jam2b* is expressed along the lateral plate mesoderm in the region that includes SVF cells. By using genetic lineage tracing and time-lapse imaging we demonstrate that *jam2b*-positive cells contribute to multiple tissues, including the mesothelium, pericardium, fin buds and venous and intestinal vasculature. To study the role of Jam2 homologs in vascular development, we have generated genetic mutants in *jam2b* and a related homolog *jam2a*. Double *jam2a; jam2b* maternal-zygotic mutants show a reduced number of SVF cells, which correlates with the defects in the formation of the intestinal and venous vasculature, and display reduced regenerative potential after endothelial cell ablation. We further demonstrate that the transcription factor *hand2* functions upstream of *jam2b* and is required for the formation of SVF cells. Altogether, our results identify a new role for Jam2 signaling and Hand2 function in the emergence of organ-specific vascular progenitors.

Results

Jam2b expression analysis

During the previous transcriptomic analysis, we have identified *jam2b* as one of the markers for SVF cells, which are late-forming vascular progenitors that emerge along the yolk extension at 24-48 hpf.[15] As we and others have previously demonstrated, *jam2b* expression is localized to the ventrolateral region of the LPM along the anterior and trunk regions during 20 somite – 48 hpf stages.[15,20,21] It is bilaterally expressed along the yolk extension during 24-48 hpf, where SVF cells

originate (Suppl. Fig. S1). We have previously demonstrated that *jam2b* and the vascular progenitor marker *etv2/etsrp* expression in the SVF cells partially overlaps along the medial portion of *jam2b* expression domain within the mid-trunk region.[15]

Generation and characterization of *jam2b*$^{Gt(2A\text{-}Gal4)}$ knock-in reporter line

To analyze *jam2b*+ cells in live embryos, we used CRISPR / Cas9-mediated non-homologous recombination approach [22] to insert Gal4 transcriptional activator into the genomic locus of *jam2b* (Suppl. Fig. S2A). Similar to the endogenous *jam2b* mRNA expression, *jam2b*$^{Gt(2A\text{-}Gal4)ci55}$*;UAS:GFP* (further abbreviated as *jam2b*$^{Gt(2A\text{-}Gal4)}$*;UAS:GFP*) expression was observed bilaterally in the lateral plate mesoderm along the yolk and yolk extension at 24 hpf (Suppl. Fig. S2B; Fig. 1A,B). At 3 and 5 dpf *jam2b*$^{Gt(2A\text{-}Gal4)}$*;UAS:GFP* expression was observed in the cell layer surrounding the yolk and yolk extension, which presumptively corresponds to the mesothelium (Fig. 1C-F). GFP expression was also observed in a subset of muscle cells within the skeletal and craniofacial muscle, and in the cells at the periphery of the eye (Fig. 1C-F). GFP expression in the trunk portion of the LPM partially overlapped with *etv2* expression in SVF cells at 30 hpf (Fig. 1G-I). Interestingly, GFP-positive cells were observed in the vasculature between 30 hpf and 3 dpf (Fig. 1J-R). The majority of GFP+ cells were located in the PCV, while a few cells were found within the ISV and SIA, and in less frequent cases contribution to the DA and parachordal lymphangioblasts (PLs) was observed (Suppl. Fig. S3). In addition, some GFP cells were located in the thoracic duct at 4 dpf, suggesting that SVF cells contribute to lymphatic vasculature (Fig. 1S-U). Due to very bright GFP expression over the yolk, we could not reliably analyze GFP cell presence in the SIV vessel, which is also positioned over the yolk and yolk extension. Overall, these findings suggest that *jam2b*+ cells contribute to the vasculature, including the PCV, ISVs, intestinal vasculature and lymphatics. These findings are consistent with our previously reported contribution of SVF cells to the PCV and intestinal vasculature [15].

Jam2b+ cells are derived from the lateral plate mesoderm and incorporate into functional vasculature

To visualize directly the contribution of *jam2b*+ cells to vasculature, we performed time-lapse imaging of *jam2b*$^{Gt(2A\text{-}Gal4)}$*;UAS:GFP*; *Tg(kdrl:mCherry)* embryos starting at 24 hpf. This imaging showed that a subset of GFP-positive cells migrated dorsally away from the LPM region, integrated into the PCV, proliferated and initiated *kdrl:mCherry* expression as they differentiated into vascular endothelial cells (Fig. 2A-F and Movie 1). This data shows that mesenchymal cells can contribute to and incorporate into the functional vasculature, even after blood circulation has initiated, in agreement with our previous observations using *etv2*$^{Gt(2A\text{-}Venus)}$ reporter line.[15]

In an attempt to identify the origin of SVF cells, we analyzed *jam2b*$^{Gt(2A\text{-}Gal4)}$*;UAS:GFP* expression at the 18-somite stage. Similar to *jam2b* mRNA expression, GFP-positive cells were located bilaterally in the lateral plate mesoderm, mostly lateral and ventral to the emerging *etv2*+ vascular progenitors (Fig. 2G-I). There was no apparent overlap between *jam2b*$^{Gt(2A\text{-}Gal4)}$*;UAS:GFP* and *etv2* expression at this stage. This domain largely overlapped with the expression domain of *prrx1a* (Fig. 2J-L), which labels the lateral portion of the LPM.[23] To analyze the behavior of these cells, we performed time-lapse imaging of *jam2b*$^{Gt(2A\text{-}Gal4)}$*;UAS:GFP* embryos starting at the 18-somite stage. GFP-positive cells remained in the same LPM region from the 18-somite stage to 24-30 hpf stages (Movie 2). As the embryo continued to undergo convergent extension, the same LPM region became bilaterally located along the yolk extension. Thus, *jam2b*-expressing cells observed at 24-30 hpf along the yolk extension are derived from the ventrolateral portion of the LPM.

Genetic lineage tracing of *jam2b*+ cells

To perform genetic lineage tracing of *jam2b*-expressing cells, we generated *UAS:Cre* and *UAS:CreERT2* zebrafish transgenic lines using Tol2 transgenesis. Subsequently they were crossed to *jam2b*$^{Gt(2A\text{-}Gal4)}$*; actb2:loxP-BFP-loxP-dsRed; fli1:GFP* adults, which ubiquitously express floxed

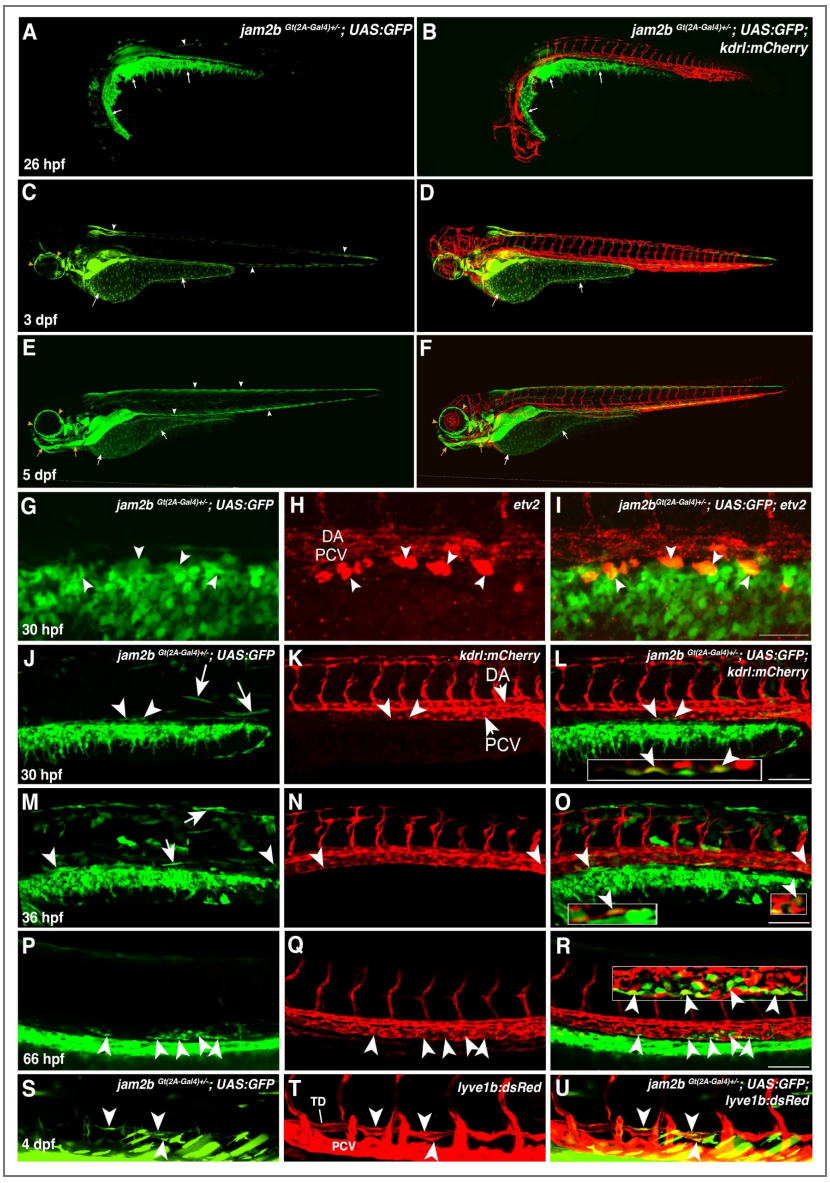

Figure 1. Characterization of *jam2b*$^{Gt(2A\text{-}Gal4)}$*;UAS:GFP* expression at 1-5 dpf.

(A-F) *jam2b*$^{Gt(2A\text{-}Gal4)}$*;UAS:GFP* shows strong GFP expression within the lateral plate mesoderm (LPM) along the yolk extension at 26 hpf (white arrows, A,B), which becomes presumptive mesothelium at 3-5 dpf (white arrows, C-F). GFP expression is also apparent in a subset of skeletal muscle cells (white arrowheads, A,C,E), craniofacial muscle (yellow arrows, E,F) and in the cells surrounding the eye (yellow arrowheads, E,F). (G-I) Co-expression of *jam2b*$^{Gt(2A\text{-}Gal4)}$*;UAS:GFP* and *etv2* (red) in the lateral plate mesoderm of the trunk region at 30 hpf. Note that GFP and *etv2* expression overlaps in the SVF cells (arrowheads), located in the most dorsal region of GFP expression domain. (J-R) Expression of *jam2b*$^{Gt(2A\text{-}Gal4)}$*;UAS:GFP* in the LPM along the yolk extension and in muscle cells from 30 to 66 hpf. A few GFP-positive cells are present in the PCV and overlap with vascular endothelial marker *kdrl:mCherry* expression (white arrowheads and insets). (S-U) Analysis of *jam2b*$^{Gt(2A\text{-}Gal4)}$*;UAS:GFP* expression in *lyve1b:dsRed* reporter background at 4 dpf, which labels PCV and the thoracic duct. Note GFP-positive cells in the TD (arrowheads). Bright GFP expression in the skeletal muscle fibers is also apparent. PCV, posterior cardinal vein; DA, dorsal aorta; TD, thoracic duct. Lateral views of the trunk region, anterior is to the left. Scale bars: 100 μm.

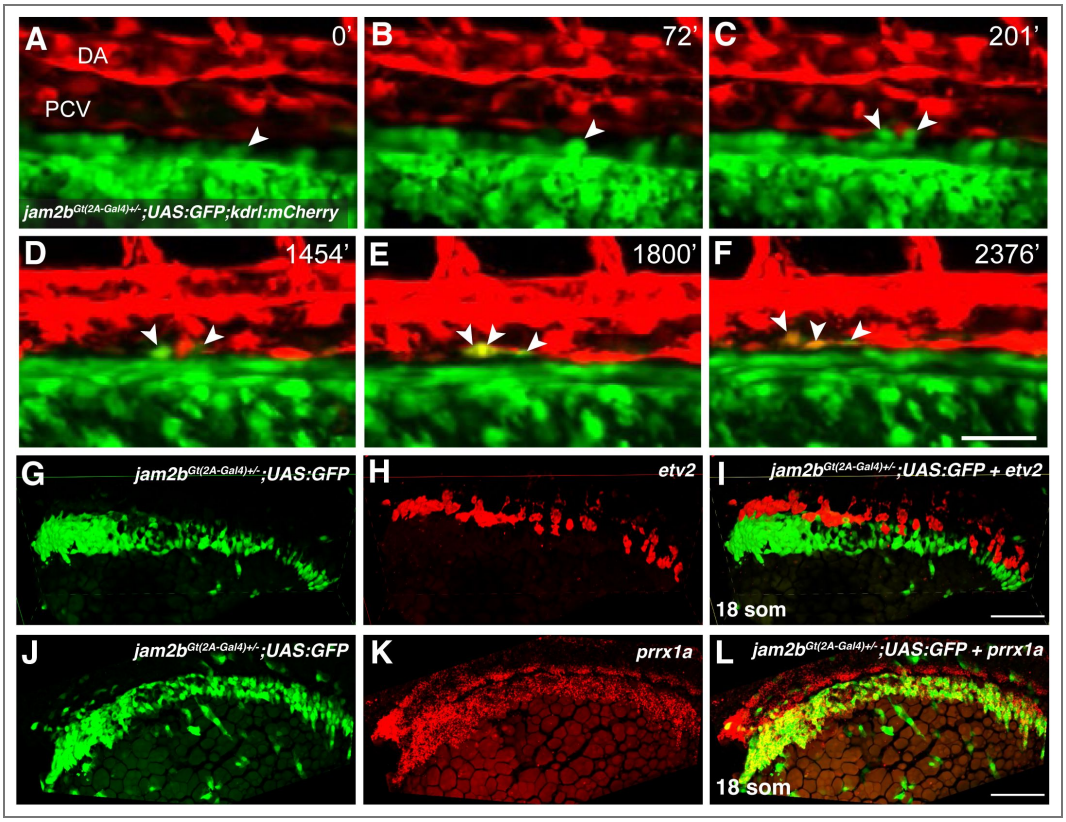

Figure 2. Jam2b-positive cells are derived from the lateral plate mesoderm and contribute to the vasculature.

(A-F) Time-lapse images of *jam2b*$^{Gt(2A\text{-}Gal4)}$*;UAS:GFP ; Tg(kdrl:mCherry)* embryo starting at 24 hpf show two GFP-positive cells (arrowheads), which migrate dorsally, proliferate, integrate into the PCV and initiate *kdrl:mCherry* expression (see Movie 1). Time is in minutes after 24 hpf. PCV, posterior cardinal vein; DA, dorsal aorta. Scale bar: 50 µm. (G-I), HCR against *etv2* in a *jam2b*$^{Gt(2A\text{-}Gal4)}$*;UAS:GFP* embryo at the 18-somite stage showing *jam2b* expression (green) lateral and ventral to *etv2* positive vascular progenitors (red). (J-L) HCR against *prrx1a* in a *jam2b*$^{Gt(2A\text{-}Gal4)}$*;UAS:GFP* embryo at the 18-somite stage showing colocalization of *prrx1a* mRNA and GFP fluorescence. Dorsolateral view of the trunk region is shown, anterior is to the left.

BFP under *actb2* promoter, in combination with the *jam2b*$^{Gt(2A\text{-}Gal4}$ knock-in driver and vascular endothelial *fli1:GFP* reporter (Fig. 3A). This approach permanently labels *jam2b*-derived cells, which switch their color from BFP to dsRed due to Cre-LoxP recombination. The embryos were then analyzed at 3 dpf by confocal microscopy, revealing switched dsRed-positive cells in the presumptive mesothelial layer surrounding the yolk and yolk extension, a subset of skeletal muscle cells and vasculature (Fig. 3B,E). In addition, both epicardial and myocardial layers within the heart were labeled by dsRed fluorescence (Fig. 3C,D). An embryo negative for *jam2b*$^{Gt(2A\text{-}Gal4)}$ expression was included for autofluorescence control (Fig. 3H). The majority of labeled vascular endothelial cells were positioned in the SIA and PCV, while a few cells were positioned in the DA, PL, and ISVs (Fig. 3F,G,I-K). Most ISVs, which showed dsRed expression, were venous, and very little contribution to arterial ISVs was observed (Fig. 3F,G,K). Due to intense dsRed fluorescence in the mesothelial layer along the yolk and yolk extension we were unable to reliably determine the contribution of *jam2b*+ cells to the SIV. To determine when *jam2b*+ cells contribute to vasculature, *UAS:CreERT2* line was crossed to *jam2b*$^{Gt(2A\text{-}Gal4)}$*; actb2:loxP-BFP-loxP-dsRed; fli1:GFP* adults and 4-hydroxitamoxifen (4-OHT) was added at different time points to induce Cre-LoxP recombination. 4-OHT addition at 7 hpf mostly in labeled SIA with a smaller fraction of cells present in the SIV, PCV and venous ISVs (Fig. 3L). Only cells in the SIA were labeled when 4-OHT was added at 22 hpf. Addition of 4-OHT at 7 hpf and subsequent washing out at 22 hpf resulted in the labeling of SIA and a small number of cells within the PCV (Fig. 3L). These results argue that *jam2b*+ cells contribute to vasculature both before and after 22 hpf. However, contribution after 22 hpf was largely limited to the intestinal vasculature, which supports our findings that SVF cells show major contribution to the SIA and SIV.

Intestinal vasculature forms largely by new vasculogenesis

Previous studies have argued that the intestinal vasculature, including the SIA and SIV, are derived from the PCV [8–10]. In contrast, our current data suggest that *jam2b*-positive SVF cells make a major contribution to the intestinal vasculature. However, the number of intestinal vascular cells labeled by *jam2b*$^{Gt(2A\text{-}Gal4)}$*; UAS:Cre* or *UAS:CreERT2* recombination was rather small. This could be due to only a small contribution of SVF cells to the intestinal vasculature, or alternatively, due to low recombination efficiency observed in *jam2b*$^{Gt(2A\text{-}Gal4)}$*; UAS:Cre* and *UAS:CreERT2* lines. To clarify the contribution of new vasculogenesis towards the intestinal vasculature, we photoconverted all vascular endothelial cells in *etv2:Kaede* transgenic line at 24 hpf stage, which expresses green to red photoconvertible Kaede in all vascular endothelial cells,[24] and then analyzed the percentage of red and green labeled cells at 4 dpf in the intestinal vasculature over the yolk extension region, where SVF cells are observed. Notably, 78.5% of cells in the SIA and 80.5% cells in the SIV showed only green expression of newly synthesized Kaede, and had no red fluorescence of photoconverted protein, arguing that they originated after photoconversion at 24 hpf stage (Fig. 4). These data suggest that most intestinal progenitors in the mid and posterior trunk regions form by new vasculogenesis from SVF cells.

Transcriptomic analysis of SVF cells

We have previously performed single-cell RNA sequencing (scRNA-seq) of the entire trunk region of zebrafish embryos in order to identify the transcriptional profile of SVF cells.[15,16] While this analysis identified a set of SVF marker genes that included *etv2, tal1, lmo2* and *jam2b*, only a limited number of marker genes were identified with this approach, because SVF cells comprise only a small portion of cells in the entire trunk. Therefore, we used *jam2b* and *etv2* reporter lines to perform additional transcriptomic analysis in order to characterize the profiles of SVF cells and their transition to vascular endothelial cells in greater detail. mCherry and Venus-positive cells were FACS-sorted from *jam2b*$^{Gt(2A\text{-}Gal4)}$*;UAS:mCherry-NTR; etv2*$^{Gt(2A\text{-}Venus}$ embryos at 36 hpf and subjected to scRNA-seq using the Chromium platform (10x Genomics). Bioinformatic analysis using Seurat 4.0 identified a total of 37 cell clusters, including the SVF cell cluster, five venous, three arterial clusters, and a capillary endothelial cluster (Fig. 5A-C, Suppl. Table 1). The SVF cell cluster (cluster #15) was identified based on top marker genes, which included *npas4l, tal1, lmo2,* and *etv2* (Fig. 5D,E, Suppl. Table 1). Additional SVF top marker genes included *gfra3, sox7,*

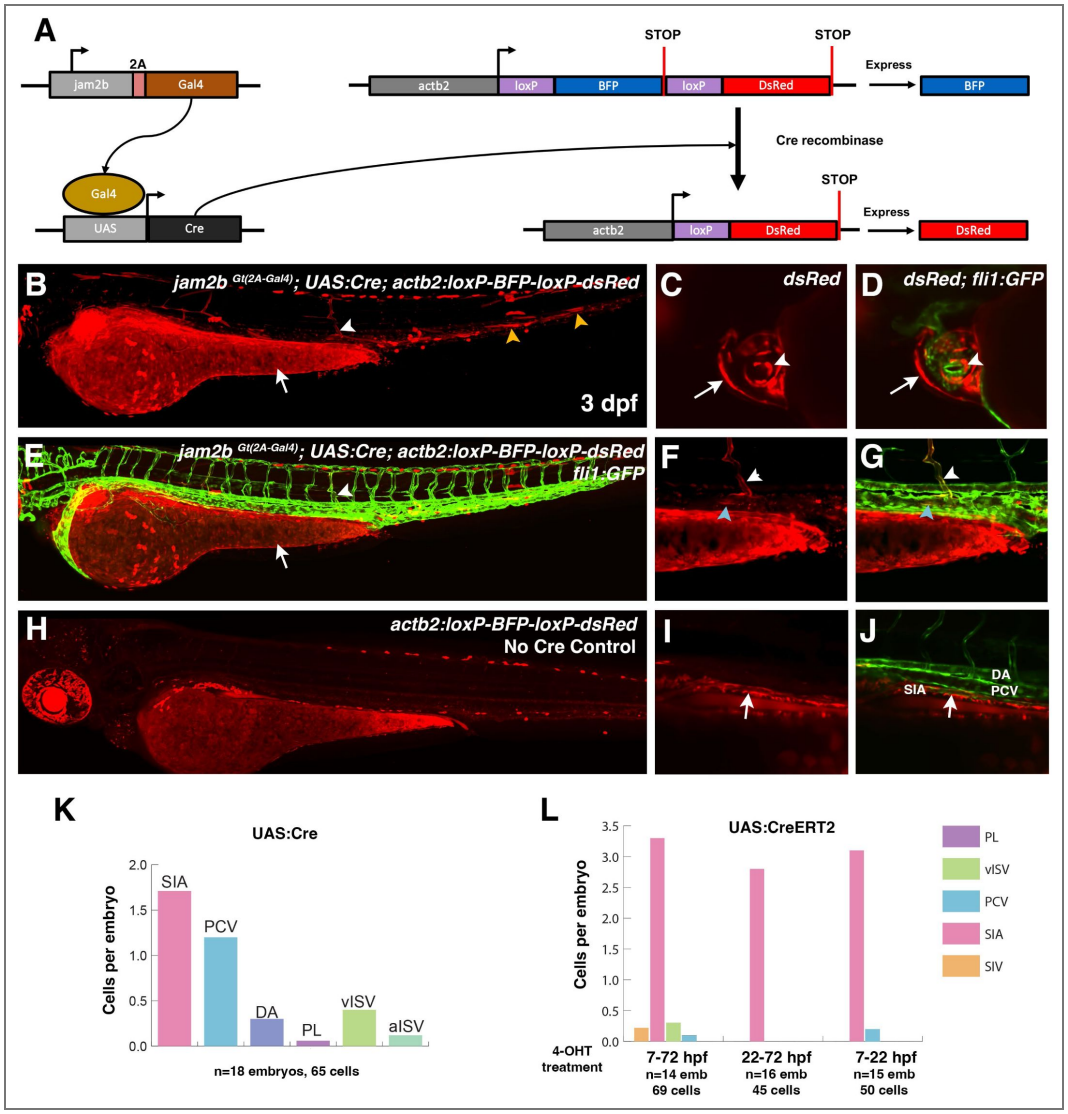

Figure 3. Genetic lineage tracing analysis of *jam2b*+ cell contribution to vasculature.

(A) Schematic diagram of recombination in *jam2b*$^{Gt(2A\text{-}Gal4)}$; *UAS:Cre; actb2-loxP-BFP-loxP-dsRed* embryos. Ubiquitous BFP expression switches to dsRed in Cre-positive cells. (B-J) Lineage tracing analysis in embryos at 3 dpf obtained by crossing *jam2b*$^{Gt(2A\text{-}Gal4)}$and *UAS:Cre; actb2:loxP-BFP-loxP-dsRed; fli1:GFP* parents. Red cells, indicating the genetic switch, are observed in the mesothelial layer surrounding the yolk (arrow, B,E), skeletal muscle (yellow arrowheads, B), and the epicardial (arrows, C,D) and myocardial (arrowheads, C,D) heart layers. Switched cells in the vasculature are observed in the venous ISVs (white arrowheads, B,E,F,G), the PCV (blue arrowheads, F,G) and SIA (arrow, I,J). A control embryo negative for *jam2b*$^{Gt(2A\text{-}Gal4)}$ is shown in (H) to indicate autofluorescence. (F,G) show larger magnification views of (B,E). (K) Quantification of endothelial cell labeling in different vascular beds in *jam2b*$^{Gt(2A\text{-}Gal4)}$; *UAS:Cre; actb2-loxP-BFP-loxP-dsRed* embryos at 3 dpf. (L) Quantification of endothelial cell labeling in different vascular beds in *jam2b*$^{Gt(2A\text{-}Gal4)}$; *UAS:CreERT2; actb2-loxP-BFP-loxP-dsRed* embryos at 3 dpf. 4-OHT was added starting at 7 hpf or 22 hpf stages. In a third group of embryos, 4-OHT was added at 7 hpf and washed out at 22 hpf stages. Note that cell contribution to SIV could not be analyzed reliably due to very strong red fluorescence in the mesothelial layer surrounding the yolk.

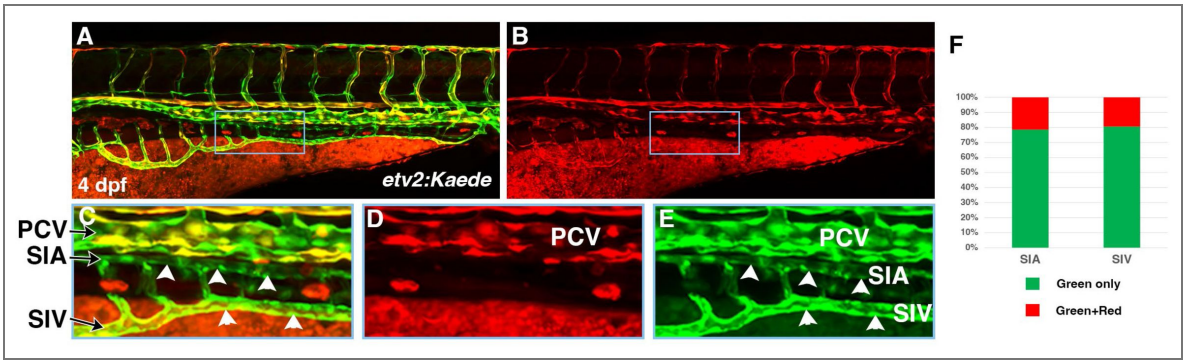

Figure 4. Intestinal vasculature in the middle and posterior trunk region forms largely by new vasculogenesis.

(A,B). *etv2:Kaede* embryos were photoconverted from green to red at 24 hpf and analyzed at 4 dpf. Merged and red only channels are shown. (C-E) Higher magnification images of the boxed area in (A,B). Merged, red and green channels are shown. Note that SIA and SIV are comprised mostly from green only cells (white arrowheads), indicating that they have originated after the photoconversion. (F) Quantification of green only (new) and green+red (pre-existing) cells in the SIA and SIV at 4 dpf. The analysis focused on the middle and posterior trunk region over the yolk extension area.

si:dkey-52l18.4, egfl7 and *tmem88a* (Suppl. Table 1). The key SVF marker genes, including *etv2, tal1, lmo2, sox7, si:dkey-52l18.4* and *egfl7* were also identified in our earlier study,[15] arguing that the current approach has successfully identified the transcriptional signature of SVF cells.

To identify transitional events during SVF cell differentiation into vascular endothelium, we performed cell lineage trajectory analysis using Monocle 3.[25] Cell lineage trajectory showed that SVF cells can directly transition into both venous and arterial clusters (Fig. 5F). Such differentiation trajectory agrees with experimental observations of SVF cells contributing both to venous (PCV, SIV) and arterial vasculature (SIA). Unfortunately, it is currently not possible to distinguish SIA or SIV-specific cells on the lineage trajectory from other types of arterial or venous cells due to the absence of specific markers for these cells.

Jam2b mutants undergo normal vascular development

To analyze the functional role of Jam2b in vascular development, we generated *jam2b* mutants using CRISPR/Cas9 mediated genome editing. Two different guide RNAs were used to delete the *jam2b* promoter region, and a stable mutant line was established (Suppl. Fig. S4A). As indicated by ISH analysis, *jam2b-/-* embryos showed no detectable *jam2b* expression in the LPM region, suggesting that the mutant may be a null or close to a null (Suppl. Fig. S4C,D). However, both zygotic and maternal zygotic *jam2b-/-* embryos appeared morphologically normal and did not show any apparent vascular defects based on *kdrl:GFP* expression analysis (data not shown). *Jam2b* homozygous mutants were viable as adults and did not exhibit any apparent defects. *Etv2* expression in SVF cells was also not affected in maternal-zygotic *jam2b* mutant embryos (Suppl. Fig. S5A-C). We have previously demonstrated that SVF cells contribute to vascular recovery after endothelial cell ablation in *etv2*$^{Gt(2A\text{-}Gal4)}$*; UAS:mCherry-NTR* embryos.[15] We then tested if vascular recovery was affected in *jam2b* deficient embryos. Metronidazole (MTZ) was added at approximately 10 hpf stage and then washed out at 45 hpf stage in zygotic *jam2b-/-* and sibling control *jam2b+/-* embryos in *etv2*$^{Gt(2A\text{-}Gal4)}$*; UAS:mCherry-NTR; kdrl:GFP* background. This resulted in nearly complete ablation of vascular endothelial cells. As we previously demonstrated, such treatment results in a complete ablation of all vascular endothelial cells except for SVF cells, which emerge later than other endothelial cells.[15] Afterwards, the recovery was analyzed at 72 hpf, when the partial regeneration of vascular cords was apparent, which as our previous study suggested, were derived from SVF cells.[15] However, no difference in vascular recovery was observed between *jam2b-/-* and *jam2b+/-* embryos (Suppl. Fig. S5D,E).

jam2a; jam2b mutants display defects in SVF cell formation and intestinal and venous vasculature

We then explored the possibility that *jam2b* may function redundantly with a related homolog *jam2a.* While *jam2a* is broadly expressed in the somitic muscle,[20,21,26] our scRNA-seq analysis indicated that it also showed significant expression in the SVF cell population, although it was not enriched among marker genes.[15] We used CRISPR / Cas9 mutagenesis to remove the entire coding sequence of *jam2a* (Suppl. Fig. S4B,E,F). To expedite the generation of double mutant embryos, *jam2a* mutant generation was performed in *jam2b-/-* mutant background. Stable *jam2a;jam2b* mutant line was generated and used for further experiments. Zygotic *jam2a-/-* / maternal *jam2b-/-* mutant embryos, obtained by the in-cross *of jam2a+/-;jam2b-/-* adults did not show any apparent defects in vascular development or SVF cell formation (data not shown). Subsequently, maternal-zygotic (MZ) mutant embryos were obtained and analyzed for SVF cell formation and vascular defects. Interestingly, MZ *jam2a-/-; jam2b-/-* embryos showed significant reduction in the SVF cell number when compared to control double heterozygous embryos in the same background. The number of *etv2, tal1* and *npas4l*-positive SVF cells was greatly reduced in MZ *jam2a;jam2b* mutant embryos, while no other morphological defects were apparent (Fig. 6). Overall vascular patterning appeared largely unaffected in MZ *jam2a;jam2b* mutant embryos based on *kdrl:GFP* fluorescence analysis at 3 dpf (Fig. 7A,B). However, MZ *jam2a;jam2b* mutant embryos showed greater incidence of incompletely extended ISVs (Fig. 7A-C). Venous ISVs, derived from the PCV, made 97% (33 out of 34) of such truncated ISVs, while only 3% were arterial. This suggested that

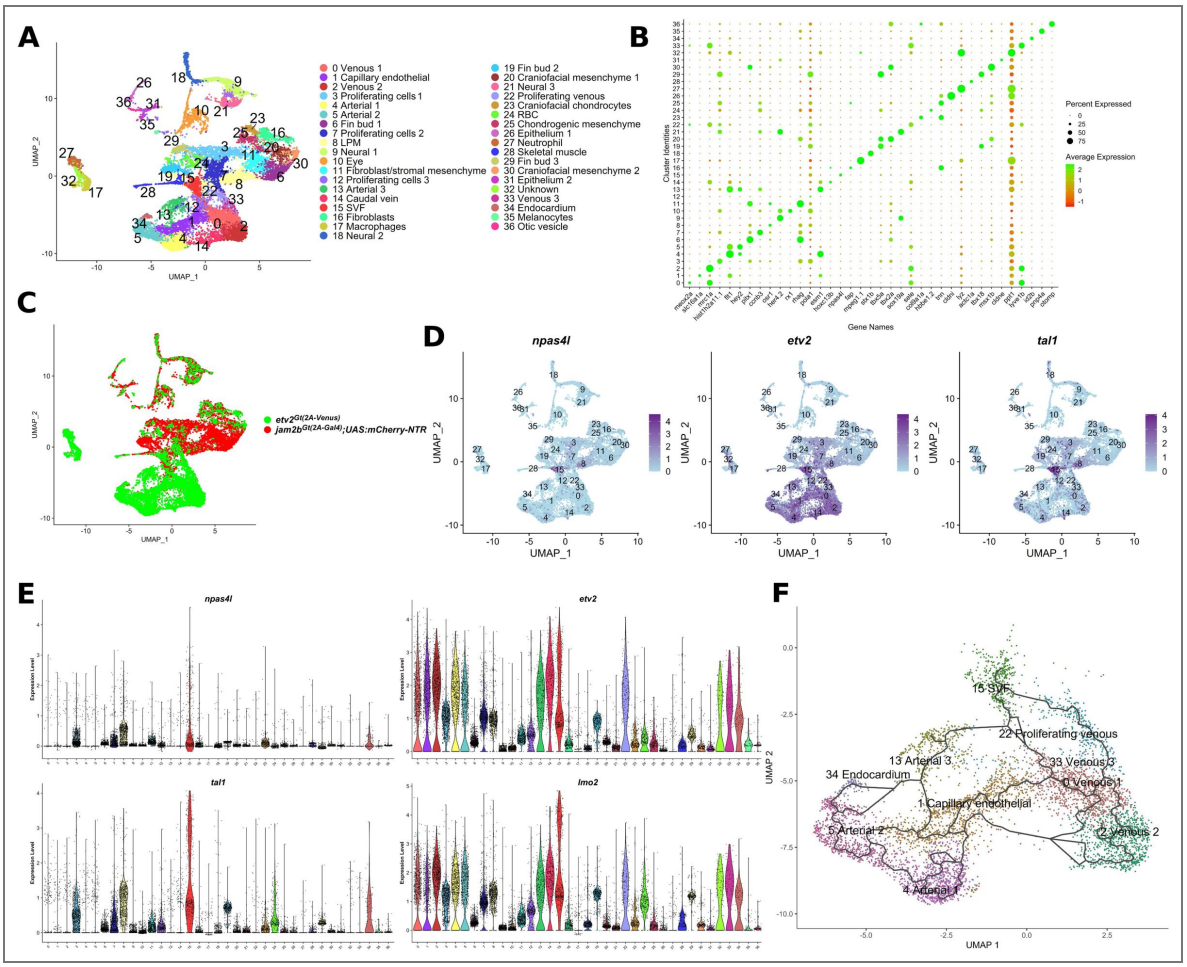

Figure 5. scRNA-seq analysis of cells from *jam2b*$^{Gt(2A-Gal4)}$;*UAS:mCherry-NTR; etv2*$^{Gt(2A-Venus)}$ embryos at 36 hpf.

(A) UMAP plot showing 37 cell clusters identified by Seurat analysis. LPM, lateral plate mesoderm; SVF, secondary vascular field; RBC, red blood cells. (B) Dot plot of selected marker gene expression level in each cell cluster. (C) 2D UMAP plot showing the distribution of Venus and mCherry positive cells. Note that Venus-positive cells mostly correspond to different vascular endothelial lineages, while mCherry-positive cells label different subsets of LPM. (D) Feature plots showing the expression of SVF cell markers, enriched in the cluster 15. (E) Violin plots show SVF cell marker expression in different clusters. (F) Pseudotime trajectory of vascular endothelial and SVF clusters made using Monocle 3. Note that SVF cells (cluster 15) can transition into both venous and arterial cell types.

the number of venous cells could be reduced, possibly due to reduced contribution of SVF cells to the PCV. Indeed, the number of ECs in the floor of the PCV was slightly yet significantly reduced in MZ *jam2a; jam2b* mutant embryos (Fig. 7D-F). However, the most pronounced defects were observed in the formation of the intestinal vasculature, in particular the SIA, which was underdeveloped and showed gaps or missing segments in MZ *jam2a;jam2b* mutants (Fig. 7G-I). In addition, a significant fraction of MZ *jam2a;jam2b* mutants showed gaps in the SIV (Fig. 7G-I).

Because our data suggested that *jam2b+* cells may contribute to lymphatics, we analyzed the formation of the thoracic duct using *prox1:RFP, fli1:GFP* reporter embryos. Approximately 37% of MZ *jam2a;jam2b* mutants had gaps in the thoracic duct compared to 5% of control *jam2a+/-;jam2b+/-* embryos (Fig. 7J-L). These results argue that *jam2a* and *jam2b* function is required for the formation of the intestinal vasculature and lymphatics.

We then tested if vascular recovery after endothelial cell ablation was affected in MZ *jam2a; jam2b* mutant embryos in *etv2*$^{Gt(2A\text{-}Gal4)}$*; UAS:mCherry-NTR* background. In order to ablate all vascular endothelial cells, MTZ was added at 6 hpf and then washed out at approximately 45 hpf. Subsequently, embryos were analyzed at 72 hpf by confocal imaging. A substantial recovery was observed in the control *jam2a; jam2b* double heterozygous embryos, while it was greatly reduced in MZ *jam2a, jam2b* mutant embryos (Fig. 7M-O). These results argue that the loss of SVF cells in MZ *jam2a; jam2b* mutants leads to defects in venous, intestinal and lymphatic vessel development, and is also associated with the reduced vascular recovery after EC ablation.

Hand2 functions upstream of *jam2b* in SVF cell formation

Recent work has identified that a bHLH transcription factor *hand2*, previously implicated in cardiac development, is also expressed in the lateral plate mesoderm along the yolk extension and labels mesothelial and pericardial progenitors, similar to *jam2b*.[27,28] Intriguingly, *hand2-2A-Cre* based lineage tracing showed contribution to the venous and intestinal vasculature,[29] similar to our results obtained using *jam2b*$^{Gt(2A\text{-}Gal4)}$*; UAS:Cre*. To determine if both genes are co-expressed in the same cells, we performed fluorescent hybridization chain reaction (HCR) analysis at 24 hpf. Indeed, expression of *hand2* and *jam2b* largely overlapped in the LPM region along the yolk extension (Fig. 8A-F). To test if *hand2* may function upstream of *jam2b*, we analyzed *jam2b* expression in the previously generated *hand2* mutants by in situ hybridization. Indeed, *jam2b* expression was absent in *hand2* mutants from most of the LPM, including the SVF-forming region along the yolk extension (Fig. 8G-J). Only the anterior domain of *jam2b* expression adjacent to the yolk was not affected in *hand2* mutants (Fig. 8G-J, white arrowheads). We then analyzed if *hand2* function is required for *etv2* expression in SVF cells. Indeed, *hand2* mutants showed complete absence of SVF cells at 30 hpf (Fig. 8K,L). In addition, *hand2* mutants showed reduced *etv2* expression in the PCV, which is consistent with its previously demonstrated requirement in the formation of venous endothelium.[30] These results argue that *hand2* functions upstream of *jam2b* in the specification of SVF cells within the trunk region of the LPM.

Discussion

Our previous work has demonstrated that new *etv2+* progenitors emerge from the trunk region of the LPM along the yolk extension and contribute to the intestinal and axial vasculature.[15] Here we implicate *jam2a* and *jam2b* function in the emergence of SVF cells and their contribution to vasculature. Our results show that *jam2b* is expressed along the broad region of LPM, including the site where SVF cells emerge. Lineage tracing studies revealed that *jam2b*-expressing cells show major contribution to the intestinal vasculature, and a smaller contribution to the PCV and venous ISVs (Fig. 9). MZ j*am2a;jam2b* mutants show a reduced number of SVF cells and display defects in the intestinal and venous vessel development. We further show that *hand2* transcription factor functions upstream of *jam2b* in the specification of SVF cells within the trunk region of the LPM.

Previous studies have argued that internal organ-specific vessels, including the intestinal vessels, are derived from the PCV.[8–10] According to the recent model, individual cells migrate and assemble into the two vessels, SIA and SIV, which can further branch and give rise to

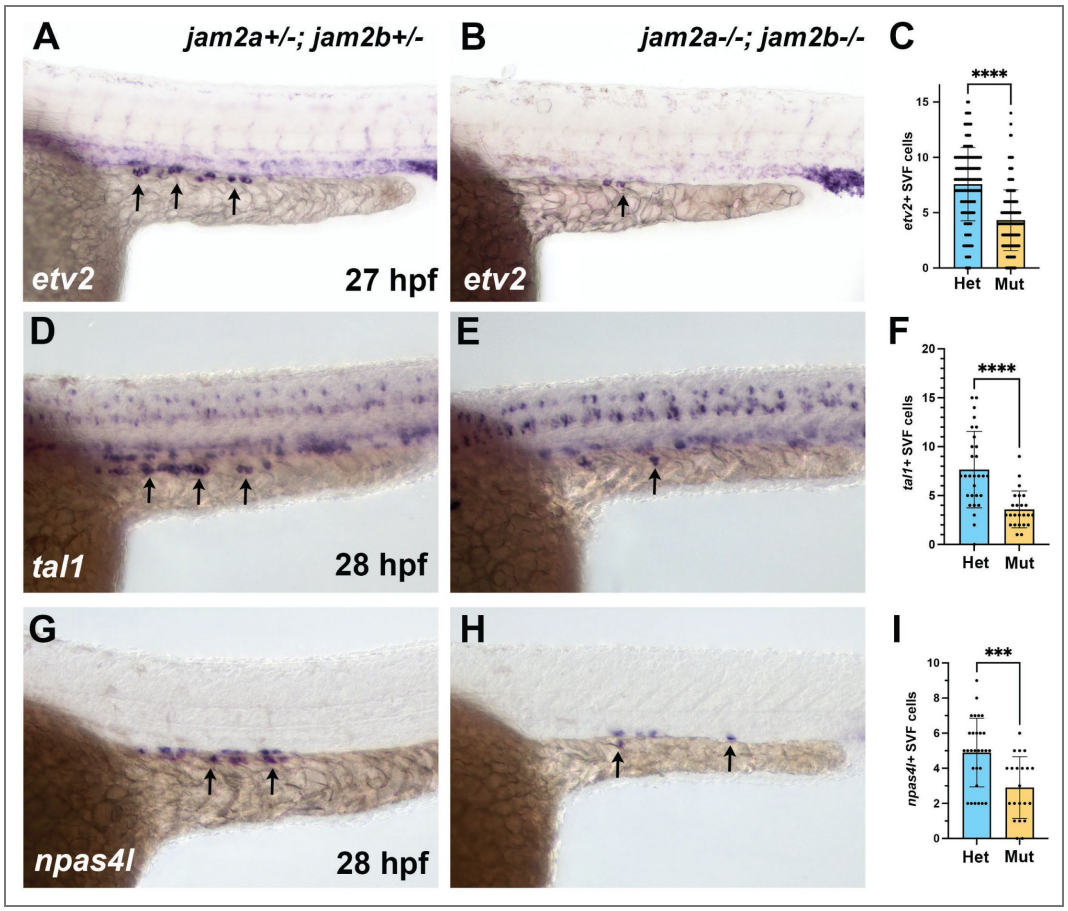

Figure 6. SVF cell number is reduced in maternal-zygotic (MZ) *jam2a; jam2b* mutant embryos.

(A-C) In situ hybridization analysis (ISH) for *etv2* expression in SVF cells (arrows, A,B) in MZ *jam2a-/-; jam2b-/-* embryos and control *jam2a+/-; jam2b+/-* embryos in *kdrl:GFP* background, obtained by crossing double homozygous *jam2a-/-; jam2b-/-; kdrl:GFP* adults to wild-type *kdrl:GFP*. (D-I) ISH analysis for *tal1* and *npas4l* expression in SVF cells (arrows) in MZ *jam2a-/-; jam2b-/-* embryos and control embryos in *fli1:GFP* background. Controls were obtained by mating *jam2a+/-; jam2b-/-* embryos to wild-type *fli1:GFP,* resulting in a mixture of *jam2a+/+; jam2b+/-* and *jam2a+/-; jam2b+/-* genotypes. ***p<0.001, ****p<0.0001, two-tailed t-test, error bars show ±s.d. Data are combined from four (C) or two (F,I) independent replicate experiments. Het labels in (C,F,I) refer to double heterozygous in (C) and a mixture of *jam2a+/+; jam2b+/-* and *jam2a+/-; jam2b+/-* genotypes in (F,I), while Mut label refers to *jam2a-/-; jam2b-/-* MZ mutant embryos.

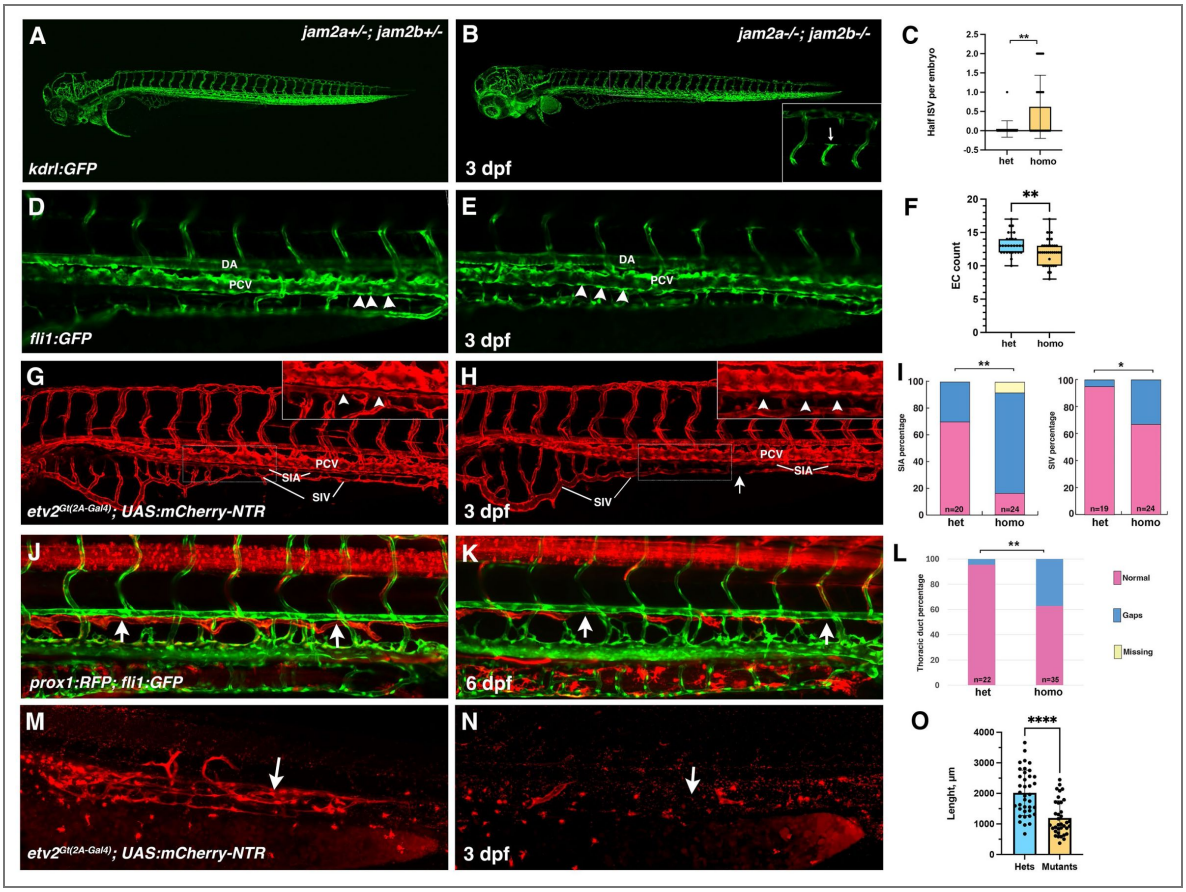

Figure 7. Analysis of vascular defects in MZ *jam2a; jam2b* mutant embryos.

(A-C) Intersegmental vessel extension analysis in MZ *jam2a-/-;jam2b-/-* and *jam2a+/-;jam2b+/-* embryos in *kdrl:GFP* background at 3 dpf. Note that some ISVs are truncated in MZ *jam2a; jam2b* mutant embryos (arrow, B, an inset shows higher magnification view of the boxed trunk region). (D-F) Endothelial cell number in the PCV is reduced in MZ *jam2a; jam2b* mutant embryos compared to *jam2a+/-;jam2b+/-* controls at 3 dpf. Endothelial cells were counted in the floor of the PCV (arrowheads) in the selected area of the trunk region based on *fli1:GFP* expression. (G-I) SIA and SIV are fragmented and show increased incidence of gaps in MZ *jam2a;jam2b* mutant embryos compared to heterozygous controls at 3 dpf. Analysis was performed in the background of *etv2*$^{Gt(2A\text{-}Gal4);}$ *UAS:mCherry-NTR* transgene, which shows expression in all vasculature. Note the underdeveloped SIA (arrowheads) and gaps in SIV (arrow) in *jam2a;jam2b* mutants. Higher magnification views are shown in the insets. Diagrams in (I) show percentage of embryos with gaps in SIA (left) and SIV (right). (J-L) Thoracic duct analysis in *prox1:RFP; fli1:GFP* transgenic embryos at 6 dpf. Note the gaps in the thoracic duct (arrows) observed in MZ *jam2a;jam2b* mutant embryos. (L) Shows the percentage of embryos with normal or fragmented thoracic duct. (M-O) Vascular recovery analysis after endothelial cell ablation. *jam2a;jam2b* mutant and control heterozygous embryos in *etv2* $^{Gt(2A\text{-}Gal4)}$*; UAS:NTR-mCherry* background were treated with MTZ starting at 6 hpf to ablate ECs and subsequently washed out at 45 hpf. A partial vascular recovery is observed in the control embryos, while it is greatly reduced in MZ *jam2a;jam2b* mutants. (O) shows length measurements of the recovered vasculature. (C,F,O) graphs show two tailed t-test, while (I,L) show Fisher's exact test. *p<0.05, **p<0.01, ****p<0.0001. DA, dorsal aorta; PCV, posterior cardinal vein; SIA, supraintestinal artery; SIV, subintestinal vein.

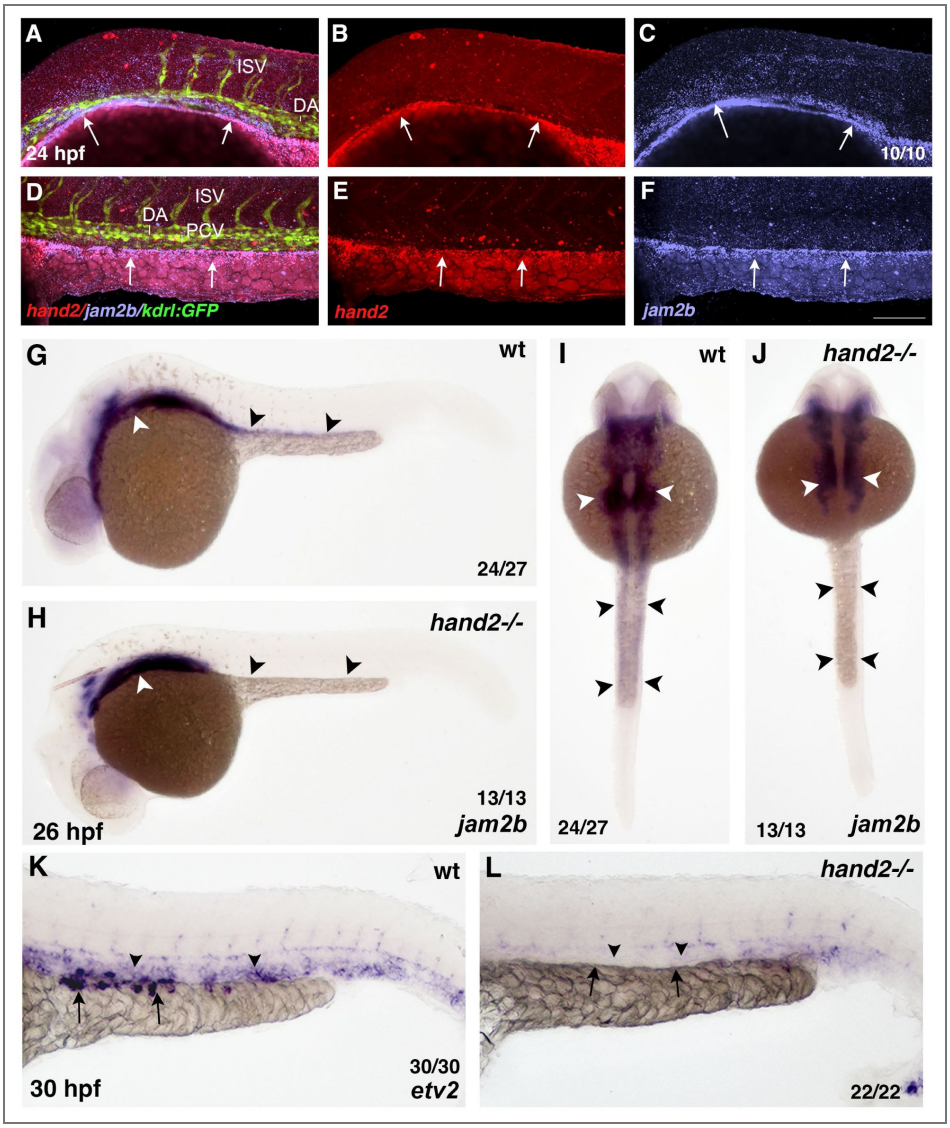

Figure 8. *hand2* is required for *jam2b* expression in the lateral plate mesoderm and SVF cells.

(A-F) HCR analysis for *hand2* (red) and *jam2b* (magenta) expression in *kdrl:GFP* embryos at 24 hpf. Anterior (A-C) and posterior (D-F) regions of the trunk are shown. Note the overlapping expression in the LPM along the yolk and yolk extension (arrows), which does not overlap with *kdrl:GFP* expression. (G-J) Whole-mount in situ hybridization analysis for *jam2b* expression in *hand2* mutant and wt control embryos at 26 hpf. Lateral (G,H) and dorsal (I,J) views. Note that *jam2b* expression in *hand2* mutants is absent from the posterior domain of the LPM along the yolk extension (black arrowheads), while the anterior portion of the LPM (white arrowheads) is only mildly affected. (K,L) Whole-mount in situ hybridization for *etv2* expression in *hand2* mutant and control wild-type embryos at 30 hpf. Note that *etv2* expression in SVF cells (arrows) is absent in *hand2* mutants. In addition, its expression in the PCV (arrowheads) is greatly reduced or absent. ISV, intersegmental vessel; DA, dorsal aorta; PCV, posterior cardinal vein. Scale bars: 100 μm.

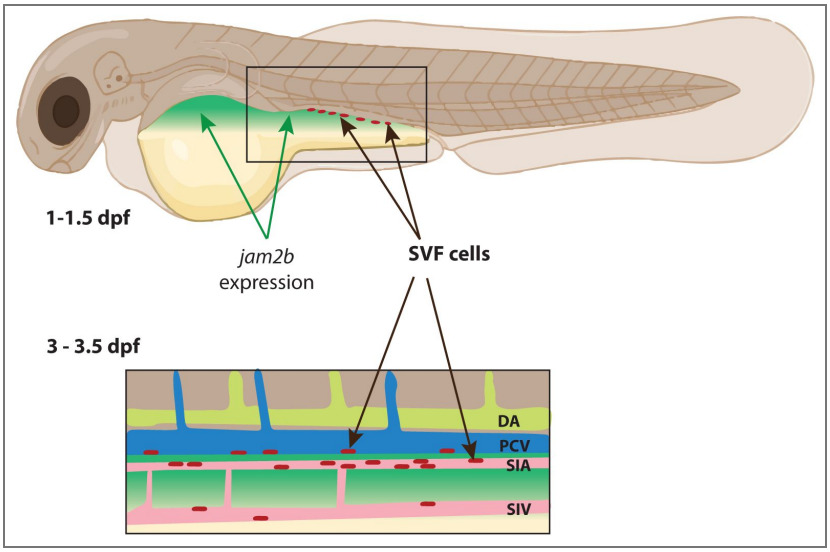

Figure 9. A diagram illustrating the emergence of SVF cells from *jam2b*-positive lateral plate mesoderm.

SVF cells contribute to the intestinal vasculature, including the supraintestinal artery (SIA), subintestinal vein (SIV), as well as the posterior cardinal vein (PCV).

interconnecting vessels, ICV.[8–10] Our recent study challenged this model and showed that SVF cells can contribute to intestinal vasculature.[15] However, it has not been clear if SVF cells have only a minor contribution to the intestinal vasculature. Our current results suggest that SVF cells may be the main source of the intestinal vasculature, while the PCV only has a minor contribution. *Etv2:Kaede* photoconversion showed that most cells in the intestinal vasculature emerge after the 24 hpf stage and, therefore, they were not present in the PCV at the time of the photoconversion. Although *jam2b*$^{Gt(2A\text{-}Gal4);}$ *UAS:Cre* based lineage tracing resulted in only a fraction of the PCV and intestinal vessels labeled with switched dsRed expression, this could be due to the relative inefficiency or mosaic expression of Cre. Based on our earlier time-lapse lineage tracing experiments, it appears that some SVF cells migrate directly to the SIA and SIV, while others integrate into the PCV first, and only afterwards exit the PCV and migrate to the intestinal vasculature.[15] Thus, our model can be reconciled with the previous observations if some SVF cells first integrate into the PCV and subsequently contribute to the intestinal vasculature. It is also possible that the earlier studies focused largely on the anterior portion of the intestinal vasculature, which forms the plexus-like structure and is largely derived from the PCV. Our study focused on the mid-trunk region along the yolk extension, where SVF cells are positioned, which is posterior to the intestinal plexus, analyzed in the previous studies.

jam2b expression within the LPM is observed during somitogenesis stages. It is evident that this region gives rise to diverse cell types, including mesothelial, pectoral fin, pericardium and muscle. Similar contribution has also been demonstrated for *hand2*-positive LPM cells,[28] which largely overlap with *jam2b* expression. Only a small fraction of *jam2b*-positive cells contributes to the vascular endothelium. The cells fated to become endothelium are located at the edge of the medial portion of the *jam2b* expression domain in the trunk region, closest to the midline (Fig. 9). It is tempting to speculate that all *jam2b* cells are multipotent initially, yet they experience different signals based on their relative position. The cells closest to the midline in the trunk region become induced to differentiate into vascular endothelium. The inductive signal is currently unknown and will require further investigation. Interestingly, *vegfaa* is expressed in the region where intestinal vessels form.[8].= Furthermore, *vegfaa* mutants show reduced number of SVF cells, which correlates with the defects in the intestinal vessel formation,[8,15] suggesting that *vegfaa* could be a candidate signal.

During embryonic vasculogenesis arterial and venous progenitors originate from the LPM during somitogenesis stages.[11–14] While the arterial progenitors originate close to the midline, venous progenitors emerge from the more lateral portion of the LPM.[24] As we show here, early venous progenitors emerge adjacent to *jam2b*-positive LPM cells, which are positioned further laterally from the venous progenitors. While *jam2b* and *etv2* expression overlaps in later forming SVF cells, it does not appear to overlap in early endothelial progenitors, which was also corroborated in our scRNA-seq data.[15,23] We also did not observe *jam2b*$^{Gt(2A\text{-}Gal4)}$*; UAS:GFP* expression in the PCV prior to 24 hpf stage, suggesting that *jam2b* may not be involved in early vasculogenesis. It appears that *jam2b*+ LPM cells maintain vasculogenic potential until later stages past 24 hpf.

The mechanism of how *jam2a; jam2b* mutants regulate SVF cell specification is unclear. A previous study has demonstrated that antibodies against murine Jam-B (Jam2) inhibited angiogenesis in vitro and interfered with the VEGFR2 signaling pathway.[31] Our previous data indicate that VEGF signaling is required to upregulate *etv2* expression during early vasculogenesis, and it is also required for SVF cell emergence.[15,32] It is possible that Jam2 signaling is required to promote VEGF signaling, which will have to be investigated in future studies.

Previous studies have demonstrated that *hand2* function is required for the PCV development. *npas4l* and *etv2* expression were reduced in the venous progenitors, arguing that *hand2* functions upstream of these transcription factors.[30,33] We show here that SVF cells are also absent in *hand2* mutants. It is possible that *hand2* directly regulates *npas4l* and /or *etv2* expression. Alternatively, *hand2* may function through *jam2b* and indirectly be involved in SVF specification through VEGF or a different pathway.

In summary, this study demonstrates that *jam2b*-positive LPM serves as a major source of internal organ-specific vascular progenitors and identifies the functional requirement for *jam2a* and *jam2b* in promoting *etv2* expression and vasculogenesis. Because analogous late-forming vascular progenitors have been also identified in the mammalian embryos,[15] it is likely that the mechanisms regulating their emergence are also evolutionarily conserved. These results will be important to understand the molecular mechanisms involved in the formation of different vascular beds and will promote the development of new approaches aimed at vascular regeneration.

Materials and methods

Zebrafish lines

The following previously established lines were used in the study: wild-type AB (Zebrafish International Resource Center), *Tg(kdrl:mCherry)*^{ci5},[34] *Tg(fli1a:GFP)*^{y1},[35] *hand2*^{s6},[27] *etv2*$^{Gt(2A\text{-}Gal4)ci32}$*;UAS:mCherry-NTR*,[36] *etv2*$^{Gt(2A\text{-}Venus)}$,[15] *Tg(actb2:loxP-BFP-loxP-dsRed)*^{sd27},[37] *Tg(kdrl:GFP)*^{s843},[14] *TgBAC(prox1a:KalT4-UAS:uncTagRFP)*^{nim5}[38] (abbreviated as *prox1:RFP*), *Tg(lyve1b:dsRed)*^{nz101}.[39]

Generation of jam2b$^{Gt(2A\text{-}Gal4)}$ knock-in line

To generate the *jam2b*$^{Gt(2A\text{-}Gal4)ci55}$*;UAS:GFP* knock-in line (further abbreviated as *jam2b*$^{Gt(2A\text{-}Gal4)}$; UAS:GFP), a gBlock Gene Fragment was made by gene synthesis (IDT) which included *jam2b* sgRNA site, the P2A sequence, *Gal4* DNA binding domain and poly-A tail. This fragment was then A-tailed using dATP and Taq DNA Polymerase (NEB, cat. no. M0273) followed by TA cloning into TOPO dual vector using manufacturer's instructions (ThermoFisher, cat. no. 450640). A mixture of 300 pg *Cas9* mRNA and 50 pg *jam2b-sgRNA-P2A-Gal4* plasmid DNA was injected into Tg(*UAS:GFP*)[40] embryos at 1-cell stage. Embryos showing any specific *GFP* expression were raised through adulthood and screened to identify a founder which produced progeny with a specific expression pattern.

Generation of jam2a and jam2b mutant lines

To generate *jam2b*^{sfl2} line, two synthetic gRNAs (Synthego) targeting *jam2b* promoter region were co-injected with Cas9 protein (NEB, EnGen Spy Cas9 NLS, Cat No. M0646) into zebrafish embryos at 1-cell stage. The following sgRNA sequences were used: GCAATTCTGGAAGAAGTCAA and AATAAGC AGGAGAAGAGCAG. Successful deletion was confirmed using the following primers outside of the deletion site: *jam2b_P3.4.5_F:* GCATCACTCAAAGGCAAATG and *jam2b_P1.2_R:* ACAGTTCCCACCATTT CAGC. A single founder with 1,071 bp deletion, which encompasses *jam2b* proximal promoter region and a portion of exon 1, was identified and used to establish the mutant line. The genomic sequence flanking the deleted region is shown here: TATAGACCGGGCAGATTAGCCATTG.....TCTTC TCCTGCTTATTTACAGTAAG.

To generate *jam2a*^{sfl3} line, two synthetic gRNAs (Synthego) were designed to delete *jam2a* coding sequence with the following sequences: TCTGTGTGCCTCTAGGTGAG and CAGAGCACAAACCCACGCA A. Both gRNAs were co-injected together with Cas9 protein into one-cell stage zebrafish embryos, homozygous for *jam2b*^{sfl2} mutation. Successful deletion was confirmed using the following primers that flank the deletion site: *jam2a-sg1_2_F:* CAAACACCTGTGACCTTACAAAA and *jam2a-sg1_2_R:* TATCAATGGCAACACAGTGG. A founder was identified with the deletion of 15,771 bp, which includes the entire *jam2a* coding sequence, and used to establish the stable line for further studies. The genomic sequence flanking the deleted region is shown here: CCTACAGGTGGTTTGTCA AGCCCAC AAAGGTAGGGAGAACATGCAAACTC

Generation of UAS:Cre and UAS:CreERT2 lines

To generate *UAS:Cre*^{sfl4} and *UAS:CreERT2*^{sfl5}lines, the gene fragment containing 5xUAS sequence, *hbae3* 5'and 3'UTR sequences, zebrafish Kozak sequence,[41] NLS-Cre, and NLS-CreERT2 codon optimized for zebrafish expression using iCodon approach,[42] SV40 polyA site, and attL4 and attL3

sequences specific to LR recombinase, was synthesized by gene synthesis and subcloned into pUC57 vector (Genscript). LR recombination into the Gateway Destination vector containing Tol2 transposase sites and lens specific alpha crystallin-dsRed sequence[43] was performed using LR recombinase (ThermoFisher). Zebrafish embryos were co-injected with 25-40pg of each construct together with 75-150 pg *tol2* mRNA. Founders were screened for the presence of lens fluorescence in their progeny. Recombination activity was tested by mating to *jam2b*$^{Gt(2A\text{-}Gal4);}$ *Tg(actb2:BFP-loxP-dsRed-loxP)* driver / reporter line. One of each lines, *UAS:Cre* and *UAS:CreERT2*, which showed good recombination activity, was selected and used for all subsequent experiments.

Confocal microscopy imaging and image processing

For confocal imaging, embryos were anesthetized in 0.016% Tricaine solution, mounted in 0.6% low melting point agarose and imaged using Nikon Eclipse or Nicon AX confocal microscope. Series of z-slices were acquired using NIS Elements software. Nikon AI Denoise function was used to reduce the image noise. Maximum intensity projection was generated using Fiji or Nikon Elements software. Images were adjusted using Levels function in Adobe Photoshop to enhance the brightness and contrast. In all cases, the same adjustments were performed in control and experimental embryo samples.

Hybridization chain reaction (HCR)

Whole mount fluorescent *in situ* hybridization was performed using the hybridization chain reaction version 3.0 as previously described.[44] Fluorescently labeled RNA probes for *etv2*, *prrx1a*, *hand2* and *jam2b* were purchased from Molecular Instruments, Inc.

Whole mount *in situ* hybridization (ISH) was performed as previously described.[45] DIG-labeled antisense RNA probes for *jam2b*,[15] *npas4l*,[15,46] *etv2/etsrp*,[47] *scl/tal1*[48] were synthesized as previously described. Following ISH, embryos were whole mounted in 0.6% low melting point agarose and imaged under light microscopy at 10X or 20X with Nikon Eclipse compound microscope. A series of z-slices were acquired using NIS Elements software to produce extended focus projected images.

4-hydroxitamoxifen (OHT) treatments

To induce tissue-specific recombination at a specific time point, *jam2b*$^{Gt(2A\text{-}Gal4)}$*;UAS:CreERT2* line was crossed with the *Tg(actb2-loxP-BFP-loxP-dsRed; fli1:GFP)* reporter line. Embryos were treated with 10 µM 4-OHT (Sigma-Aldrich) solution starting at 7 or 22 hpf stage. Alternatively, to analyze the timing requirement, embryos were treated at 7 hpf stage and subsequently washed at 22 hpf by rinsing a few times in embryo water. Confocal z-stacks were acquired at 3 dpf and analyzed with NIS Elements Software. Recombination was quantified by counting dsRed-positive cells within vasculature.

Endothelial cell (EC) count

To assess EC number in *jam2a;jam2b* double homozygous mutants and control heterozygous embryos, confocal images were analyzed using NIS Elements Imaging Software. An area consisting of 5 intersegmental vessels in the trunk region was selected, and ECs located at the bottom of the posterior cardinal vein (PCV) were manually counted.

Subintestinal vessel and thoracic duct (TD) measurements

To evaluate SIA, SIV and TD in *jam2a; jam2b* double homozygous mutants and control heterozygous embryos, confocal images were analyzed using NIS Elements 5.41.02 Imaging Software. SIA, SIV and TD were categorized into normal and abnormal groups according to morphological characteristics. Normal vessels were considered uniform and without any gaps throughout the whole embryo; everything else was considered abnormal.

Chemical cell ablation

To assess vascular tissue ablation and regeneration, *jam2a;jam2b* homozygous mutant zebrafish in *kdrl:GFP* background were crossed with *jam2a;jam2b* homozygous mutants carrying the $etv2^{Gt(2A\text{-}Gal4)}$*; UAS:NTR-mCherry* transgene. As a control group, heterozygous embryos were obtained by crossing *jam2a; jam2b* homozygous mutants carrying the $etv2^{Gt(2A\text{-}Gal4)}$*; UAS:NTR-mCherry* transgene with wild-type *kdrl:GFP*. Embryos were collected and treated with 10 mM metronidazole (MTZ) dissolved in 0.1 % DMSO at 6 or 10 hpf stages. At 2 dpf, embryos were dechorionated, thoroughly washed, and transferred to fresh embryo water to allow for recovery. Confocal imaging was performed at 3 dpf to assess vascular regeneration. NIS-Elements Imaging Software (version 5.41.02) was used to quantify tissue ablation and recovery. The total length of regenerated vessels was calculated by measuring and adding the lengths of all recovered vessels based on mCherry and GFP expression.

Statistical analysis

Data representing graphs were generated and statistical analyses (t-test and Fisher's exact test) were performed using GraphPad Prism software.

Single-cell RNA-seq analysis

Transgenic $etv2^{Gt(2A\text{-}Venus)}$ fish were crossed to $jam2b^{Gt(2A\text{-}Gal4)}$*;UAS:NTR-mCherry* fish. Double-positive embryos expressing both *Venus* and *mCherry* fluorescent proteins were selected at 36 hpf. Embryos were dechorionated and immediately transferred into a 1.5 ml Eppendorf tube for the generation of single-cell suspension. Whole embryos were then dissociated into a single-cell suspension by cold protease tissue dissociation protocol [49]. Cells expressing *Venus* only, *mCherry* only, and both (*Venus* and *mCherry*) were sorted using a BD/FACSAria II flow cytometer cell sorter. After sorting, cells expressing both *Venus* and *mCherry* were equally divided and added into the *Venus* only and *mCherry* only populations manually. Suspensions of ~10,000 single Venus and mCherry-positive cells were loaded separately onto the 10XGenomics Single Cell 3' (V3 chemistry) chip. 12 cDNA amplification cycles were used to generate cDNA. Samples were sequenced on an Illumina NovaSeq 6000 instrument (Illumina, San Diego, CA) running an S2 flow cell with parameters as follows: Read1, 28 cycles; Index Read1: 8 cycles; Read 2: 91 cycles at the CCHMC DNA Sequencing core. The fastq files obtained from the sequencing core were then mapped to the Danio rerio genome (version zv11) to generate single-cell feature counts using Cell Ranger version 3.0.2. Counts were generated using fastq files from each of the populations individually. Utilizing R packages: Seurat,[50] ggplot2,[51] dplyr,[52] reshape2,[53] and tidyverse[54] the data was filtered for high quality cells with 200-3500 features and less than 5% mitochondrial gene content. The datasets were then integrated and the figure plots were made using custom written R code.[55–57] To find a stable cluster resolution we tested resolutions between 0-3 in 0.1 increments and decided on 1.6, revealing the SVF cells in cluster 15. We then selected clusters for trajectory analysis using the Monocle3 package. The UMAP, feature plots, and violin plots were made using Seurat, and the lineage plot was made using Monocle3.[25] Cluster annotation was done manually based on the top marker gene expression. In some cases, AI ChatGPT 5 assistance was used to help with the cell type prediction based on 40-60 top marker gene expression, which was subsequently verified manually based on published gene expression patterns. Single-cell RNA-seq dataset has been submitted to NCBI GEO database under accession number: GSE179926.

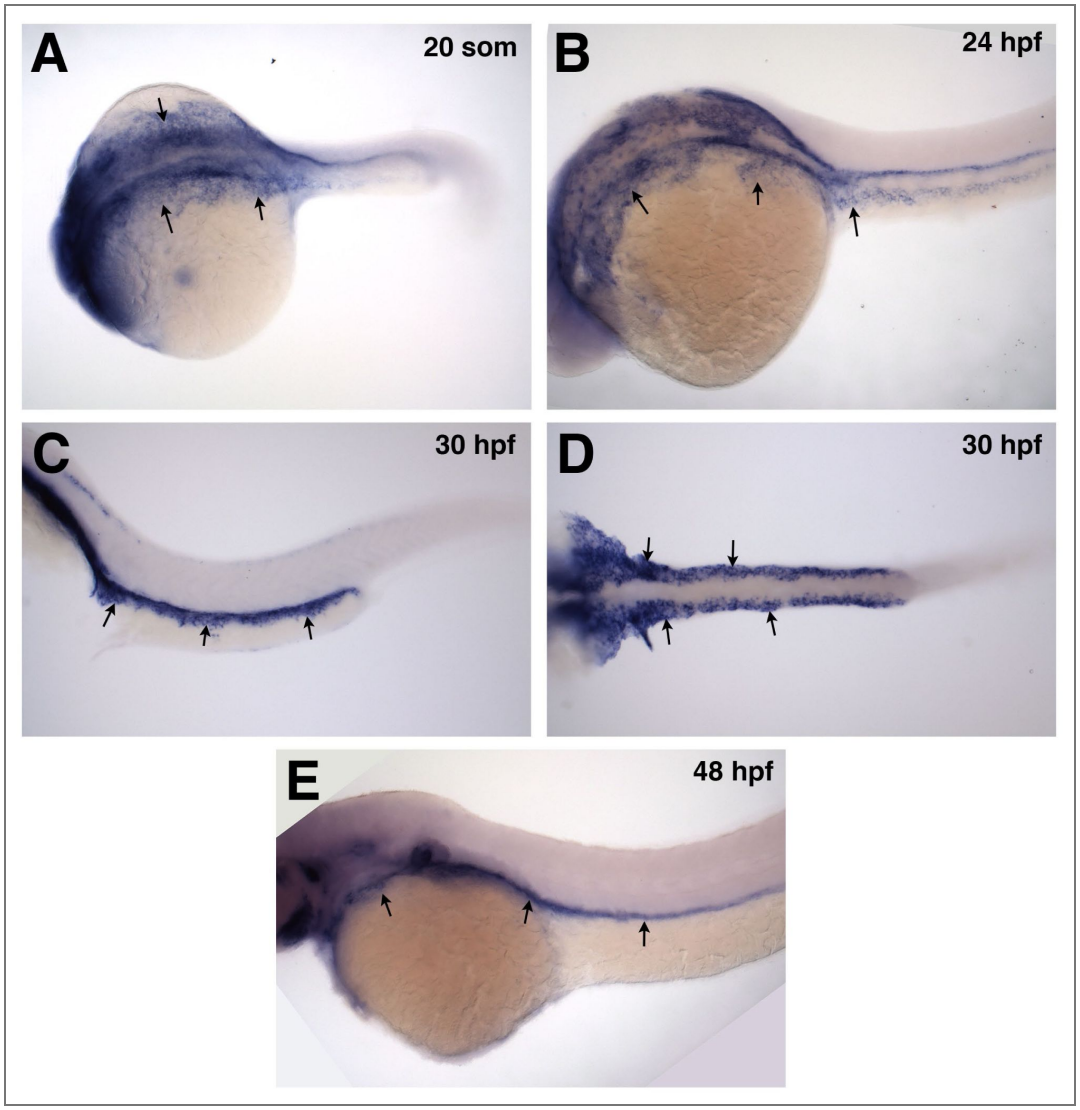

Supplementary Figure S1. In situ hybridization analysis of *jam2b* expression between the 20-somite and 48 hpf stages. Note strong *jam2b* expression in the lateral plate mesoderm along the yolk and yolk extension (arrows). (A,B,C,E) lateral view, (D) ventral view.

Supplementary Figure S2. Generation of *jam2b*$^{Gt(2A\text{-}Gal4)}$*;UAS:GFP* line using CRISPR-Cas9 mediated non-homologous recombination.

(A) A diagram of *sgRNA-2A-Gal4* construct and its insertion into the *jam2b* genomic locus. The targeting construct contained *jam2b* sgRNA site, followed by in-frame fusion to the viral peptide P2A, Gal4 DNA-binding domain and the SV40 polyA sequence. *jam2b* sgRNA targets the second exon of *jam2b* genomic sequence. (B) Comparison of GFP fluorescence in *jam2b*$^{Gt(2A\text{-}Gal4)}$*;UAS:GFP* embryo and *jam2b* mRNA expression analyzed by in situ hybridization at 24 hpf. Note the bilateral *jam2b* expression and GFP fluorescence observed in the lateral mesoderm along the yolk and yolk extension. Scale bars: 100 μm.

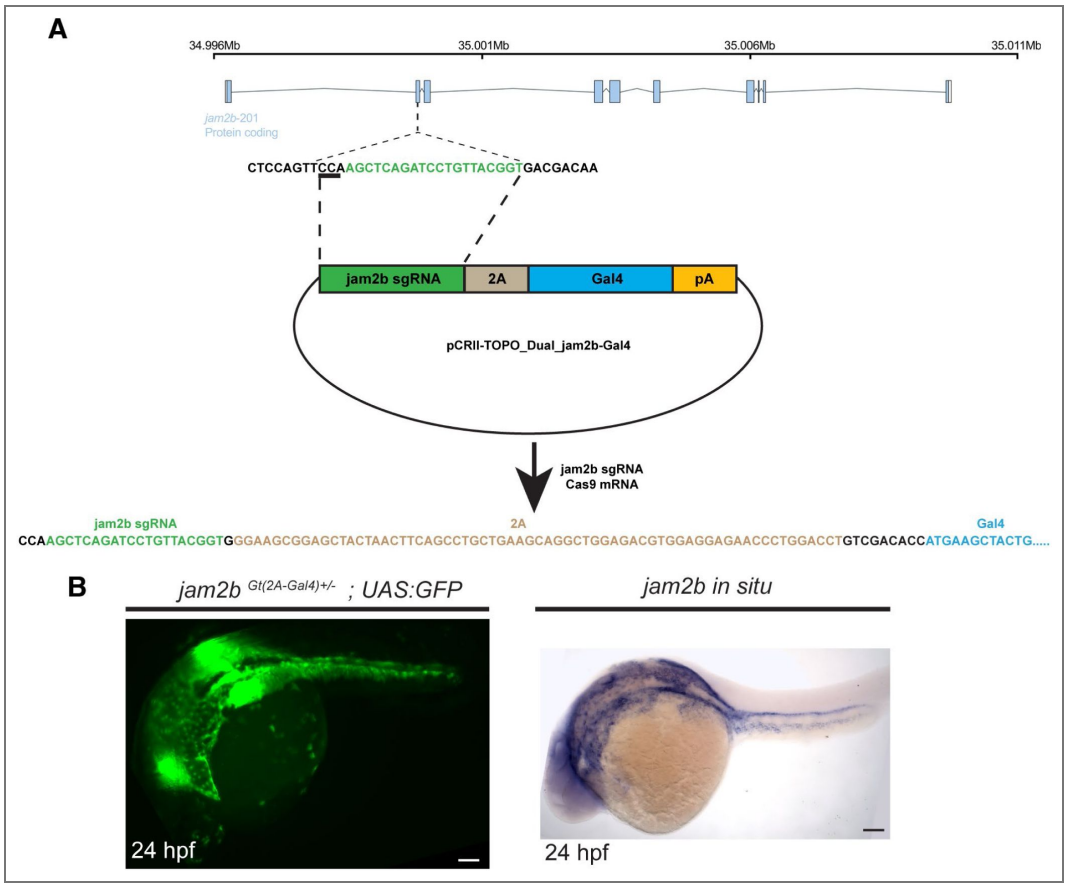

Supplementary Figure S3. Quantification of *jam2b*$^{Gt(2A\text{-}Gal4)}$*;UAS:GFP* cell contribution to different vascular beds.

All analysis at 3 dpf, except for TD, which is at 4 dpf. n=7 embryos except for TD, for which n=17. PCV, posterior cardinal vein, DA, dorsal aorta, ISV, intersegmental vessel, PL, parachordal lymphangioblast, SIA, supraintestinal artery, TD, thoracic duct.

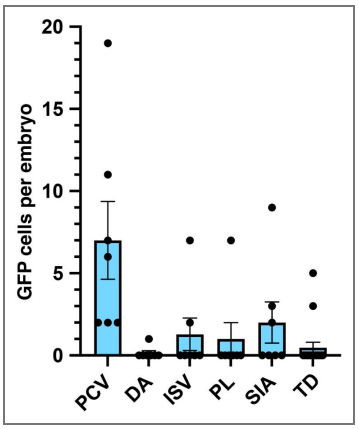

Supplementary Figure S4. Generation of *jam2b* and *jam2a* mutants using CRISPR-Cas9 genome editing.

(A) A schematic diagram illustrating generation of *jam2b* mutants using two sgRNAs designed to delete the promoter region. (B) A schematic diagram illustrating generation of *jam2a* mutants using two sgRNAs designed to delete the entire *jam2a* coding sequence. (C,D) In situ hybridization (ISH) analysis for *jam2b* expression in wild-type *jam2b+/+* and *jam2b-/-* mutant embryos at 30 hpf. Note that *jam2b* expression along the lateral plate mesoderm is absent in *jam2b* mutants (arrows). Some residual staining is due to background and some pigment cells along the horizontal myoseptum. (E,F) ISH analysis for *jam2a* expression in wild-type *jam2a+/+* and *jam2a-/-* mutants at 26 hpf. The strongest *jam2a* expression is observed in the posterior somites, which is absent in *jam2a* mutants (arrows).

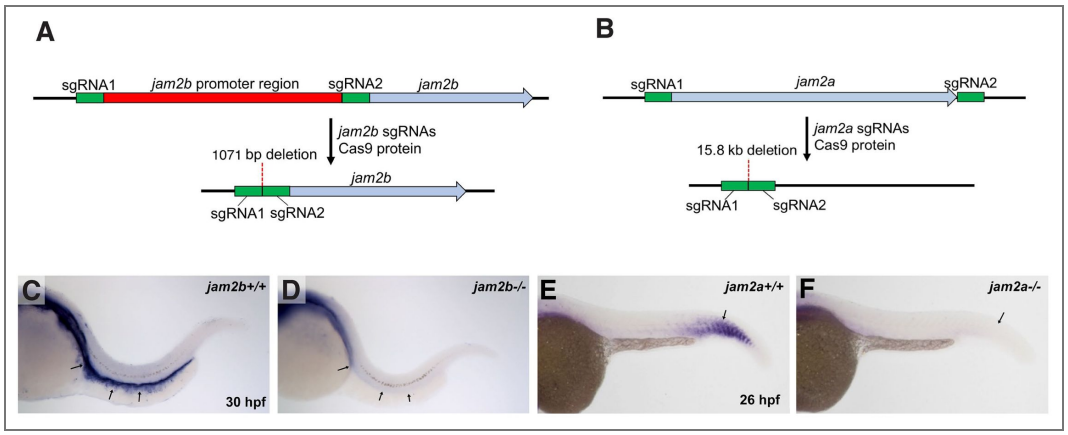

Supplementary Figure S5. *jam2b* mutant embryos do not show any apparent defects in SVF cell formation or vascular recovery after endothelial cell ablation.

(A-C) Quantification of SVF cells (white arrowheads) by in situ hybridization analysis for *etv2* expression at 30 hpf. Experimental and control embryos were obtained from the incross of *jam2b-/-* or wild-type (*jam2b+/+*) sibling parents in *kdrl:GFP* background, respectively. (D,E) Quantification of vascular recovery after endothelial cell ablation. *jam2b+/-* and *jam2b-/-* adults in *etv2*$^{Gt(2A\text{-}Gal4)}$*; UAS:mCherry-NTR; Tg(kdrl:GFP)* background were crossed with each other. Embryos were treated with 10mM MTZ from 10 hpf to 45 hpf, which was then washed and embryos were allowed to undergo vascular recovery until 72 hpf, when they were imaged and genotyped. Control embryos were treated with 0.1% DMSO. The length of new vascular cords (white lines) at the position of the PCV and SIV was measured and compared in *jam2b+/-* and *jam2b-/-* mutant embryos. Note that the bright *kdrl:GFP* expression along the yolk extension corresponds to the pronephros and was not affected in these experiments. Lateral view is shown, anterior is to the left. Mean±sd is shown; ns, not significant. Scale bars: 100 µm.

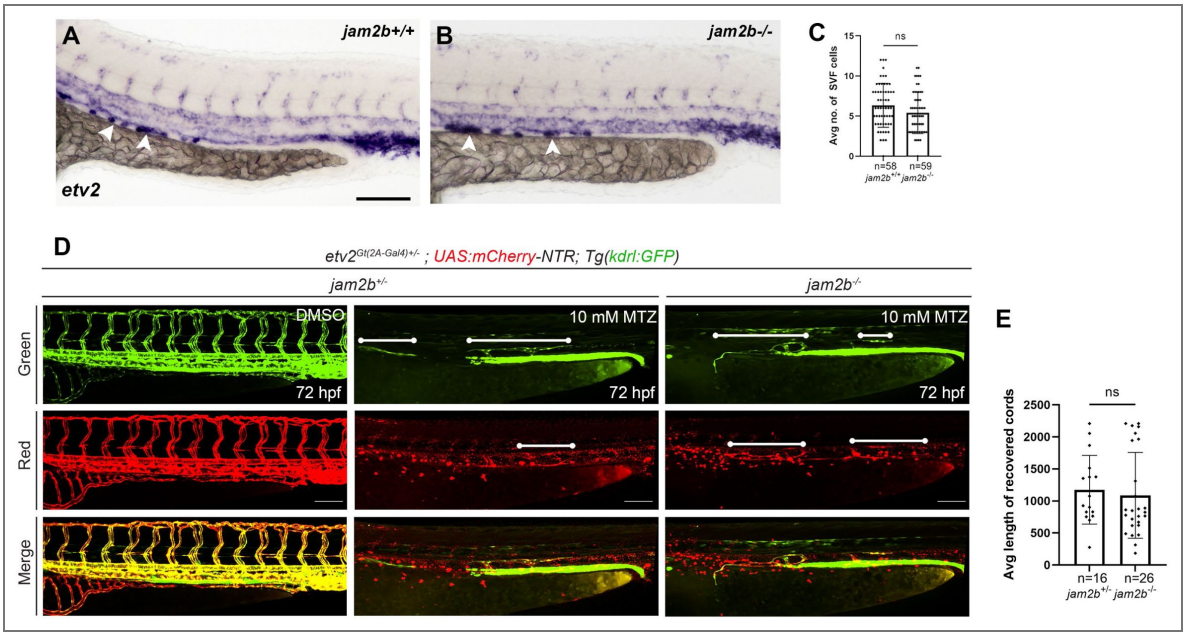

Acknowledgements

This research was supported by NIH R01 HL153005 to S.S., a supplemental postdoctoral diversity award R01 HL163161-S1 to R.D., AHA 19POST34400016 award to S.M. and AHA 19POST34450021 award to S.G. We thank Olivia Nester and Kanwal Jussa for their assistance with zebrafish experiments.

Additional information

Data availability

scRNA-seq data were deposited in NCBI GEO (accession number GSE179926). All data generated or analyzed during this study are included in the manuscript and supporting files.

Funding

Funder	Grant reference number	Author
HHS | National Institutes of Health (NIH)	HL153005	Saulius Sumanas
HHS | National Institutes of Health (NIH)	HL163161-S1	Saulius Sumanas
American Heart Association (AHA)	19POST34400016	Sanjeeva Metikala
American Heart Association (AHA)	19POST34450021	Suman Gurung

Author ORCID iDs

Saulius Sumanas: https://orcid.org/0000-0002-8605-6122

Additional files

Supplemental Table 1

Movie 1. >Migration of *jam2b*-expressing cells from the lateral plate mesoderm into the PCV. A time-lapse video of a *jam2b*$^{Gt(2A\text{-}Gal4)}$*;UAS:GFP;Tg(kdrl:mCherry)* embryo shows GFP positive cells migrating dorsally, integrating into the PCV, proliferating and initiating *kdrl:mCherry* expression (white arrowheads) (see Fig. 2A-F). Imaging was started at 24 hpf. PCV, posterior cardinal vein; DA, dorsal aorta. Scale bar: 20 μm.

Movie 2. *jam2b*-expressing cells are derived from the lateral plate mesoderm. A time-lapse video of a *jam2b*$^{Gt(2A\text{-}Gal4)}$*;UAS:GFP;Tg(kdrl:mCherry)* embryo showing from the 18-somite stage to 24 hpf. GFP positive cells can be seen in the ventrolateral LPM region at the 18-somite stage and remain in the same region until 24 hpf as the embryo undergoes convergent extension. PCV, posterior cardinal vein; DA, dorsal aorta. Scale bar: 50 μm.

References

1. **Gouysse G.,** Couvelard A., Frachon S., Bouvier R., Nejjari M., Dauge M.C., Feldmann G., Henin D., Scoazec J.Y (2002) Relationship between vascular development and vascular differentiation during liver organogenesis in humans. *J Hepatol* **37**:730-740 https://doi.org/10.1016/s0168-8278(02)00282-9
2. **Kingsbury J.W.,** Alexanderson M., Kornstein E.S (1956) The development of the liver in the chick. *Anat Rec* **124**:165-187 https://doi.org/10.1002/ar.1091240204
3. **Matsumoto K.,** Yoshitomi H., Rossant J., Zaret K.S (2001) Liver organogenesis promoted by endothelial cells prior to vascular function. *Science* **294**:559-563 https://doi.org/10.1126/science.1063889
4. **Sherer G.K.** (1991) *The Development of the Vascular System* Karger.

5. **Goldman O.,** Han S., Hamou W., Jodon de Villeroche V., Uzan G., Lickert H., Gouon-Evans V. (2014) Endoderm generates endothelial cells during liver development. *Stem Cell Reports* **3**:556-565 https://doi.org/10.1016/j.stemcr.2014.08.009

6. **Perez-Pomares J.M.,** Carmona R., Gonzalez-Iriarte M., Macias D., Guadix J.A., Munoz-Chapuli R (2004) Contribution of mesothelium-derived cells to liver sinusoids in avian embryos. *Dev Dyn* **229**:465-474 https://doi.org/10.1002/dvdy.10455

7. **Zhang H.,** Pu W., Tian X., Huang X., He L., Liu Q., Li Y., Zhang L., He L., Liu K., *et al.* (2016) Genetic lineage tracing identifies endocardial origin of liver vasculature. *Nat Genet* **48**:537-543 https://doi.org/10.1038/ng.3536

8. **Koenig A.L.,** Baltrunaite K., Bower N.I., Rossi A., Stainier D.Y., Hogan B.M., Sumanas S (2016) Vegfa signaling promotes zebrafish intestinal vasculature development through endothelial cell migration from the posterior cardinal vein. *Dev Biol* **411**:115-127 https://doi.org/10.1016/j.ydbio.2016.01.002

9. **Goi M.,** Childs S.J (2016) Patterning mechanisms of the sub-intestinal venous plexus in zebrafish. *Dev Biol* **409**:114-128 https://doi.org/10.1016/j.ydbio.2015.10.017

10. **Hen G.,** Nicenboim J., Mayseless O., Asaf L., Shin M., Busolin G., Hofi R., Almog G., Tiso N., Lawson N.D., *et al.* (2015) Venous-derived angioblasts generate organ-specific vessels during zebrafish embryonic development. *Development* **142**:4266-4278 https://doi.org/10.1242/dev.129247

11. **Eriksson J.,** Lofberg J (2000) Development of the hypochord and dorsal aorta in the zebrafish embryo (Danio rerio). *J Morphol* **244**:167-176 https://doi.org/10.1002/(SICI)1097-4687(200006)244:3<167::AID-JMOR2>3.0.CO;2-J

12. **Fouquet B.,** Weinstein B.M., Serluca F.C., Fishman M.C (1997) Vessel patterning in the embryo of the zebrafish: guidance by notochord. *Dev Biol* **183**:37-48 https://doi.org/10.1006/dbio.1996.8495

13. **Childs S.,** Chen J.N., Garrity D.M., Fishman M.C (2002) Patterning of angiogenesis in the zebrafish embryo. *Development* **129**:973-982 https://doi.org/10.1242/dev.129.4.973

14. **Jin S.W.,** Beis D., Mitchell T., Chen J.N., Stainier D.Y (2005) Cellular and molecular analyses of vascular tube and lumen formation in zebrafish. *Development* **132**:5199-5209 https://doi.org/10.1242/dev.02087

15. **Metikala S.,** Warkala M., Casie Chetty S., Chestnut B., Rufin Florat D., Plender E., Nester O., Koenig A.L., Astrof S., Sumanas S (2022) Integration of vascular progenitors into functional blood vessels represents a distinct mechanism of vascular growth. *Dev Cell* **57**:767-782.e766. https://doi.org/10.1016/j.devcel.2022.02.015

16. **Metikala S.,** Casie Chetty S., Sumanas S (2021) Single-cell transcriptome analysis of the zebrafish embryonic trunk. *PLoS One* **16**:e0254024 https://doi.org/10.1371/journal.pone.0254024

17. **Ebnet K** (2017) Junctional Adhesion Molecules (JAMs): Cell Adhesion Receptors With Pleiotropic Functions in Cell Physiology and Development. *Physiol Rev* **97**:1529-1554 https://doi.org/10.1152/physrev.00004.2017

18. **Kobayashi I.,** Kobayashi-Sun J., Hirakawa Y., Ouchi M., Yasuda K., Kamei H., Fukuhara S., Yamaguchi M (2020) Dual role of Jam3b in early hematopoietic and vascular development. *Development* **147** https://doi.org/10.1242/dev.181040

19. **Kobayashi I.,** Kobayashi-Sun J., Kim A.D., Pouget C., Fujita N., Suda T., Traver D (2014) Jam1a-Jam2a interactions regulate haematopoietic stem cell fate through Notch signalling. *Nature* **512**:319-323 https://doi.org/10.1038/nature13623

20. **Powell G.T.,** Wright G.J (2012) Genomic organisation, embryonic expression and biochemical interactions of the zebrafish junctional adhesion molecule family of receptors. *PLoS One* **7**:e40810 https://doi.org/10.1371/journal.pone.0040810

21. **Thisse B.,** Thisse C. (2004) Fast Release Clones: A High Throughput Expression Analysis. ZFIN.

22. **Auer T.O.,** Duroure K., De Cian A., Concordet J.P., Del Bene F. (2014) Highly efficient CRISPR/Cas9-mediated knock-in in zebrafish by homology-independent DNA repair. *Genome Res* **24**:142-153 https://doi.org/10.1101/gr.161638.113

23. **Chestnut B.,** Casie Chetty S., Koenig A.L., Sumanas S (2020) Single-cell transcriptomic analysis identifies the conversion of zebrafish Etv2-deficient vascular progenitors into skeletal muscle. *Nat Commun* **11**:2796 https://doi.org/10.1038/s41467-020-16515-y

24. **Kohli V.,** Schumacher J.A., Desai S.P., Rehn K., Sumanas S (2013) Arterial and venous progenitors of the major axial vessels originate at distinct locations. *Dev Cell* **25**:196-206 https://doi.org/10.1016/j.devcel.2013.03.017

25. **Cao J.,** Spielmann M., Qiu X., Huang X., Ibrahim D.M., Hill A.J., Zhang F., Mundlos S., Christiansen L., Steemers F.J., *et al.* (2019) The single-cell transcriptional landscape of mammalian organogenesis. *Nature* **566**:496-502 https://doi.org/10.1038/s41586-019-0969-x

26. **Powell G.T.,** Wright G.J (2011) Jamb and jamc are essential for vertebrate myocyte fusion. *PLoS Biol* **9**:e1001216 https://doi.org/10.1371/journal.pbio.1001216

27. **Yelon D.,** Ticho B., Halpern M.E., Ruvinsky I., Ho R.K., Silver L.M., Stainier D.Y (2000) The bHLH transcription factor hand2 plays parallel roles in zebrafish heart and pectoral fin development. *Development* **127**:2573-2582 https://doi.org/10.1242/dev.127.12.2573

28. **Prummel K.D.,** Crowell H.L., Nieuwenhuize S., Brombacher E.C., Daetwyler S., Soneson C., Kresoja-Rakic J., Kocere A., Ronner M., Ernst A., *et al.* (2022) Hand2 delineates mesothelium progenitors and is reactivated in mesothelioma. *Nat Commun* **13**:1677 https://doi.org/10.1038/s41467-022-29311-7

29. **Ming Z.,** Liu F., Moran H.R., Lalonde R.L., Adams M., Restrepo N.K., Joshi P., Ekker S.C., Clark K.J., Friedberg I., *et al.* (2025) Lineage labeling with zebrafish hand2 Cre and CreERT2 recombinase CRISPR knock-ins. *Dev Dyn* **255**:86-105 https://doi.org/10.1002/dvdy.70022

30. **Perens E.A.,** Garavito-Aguilar Z.V., Guio-Vega G.P., Pena K.T., Schindler Y.L., Yelon D (2016) Hand2 inhibits kidney specification while promoting vein formation within the posterior mesoderm. *eLife* **5** https://doi.org/10.7554/eLife.19941

31. **Meguenani M.,** Miljkovic-Licina M., Fagiani E., Ropraz P., Hammel P., Aurrand-Lions M., Adams R.H., Christofori G., Imhof B.A., Garrido-Urbani S (2015) Junctional adhesion molecule B interferes with angiogenic VEGF/VEGFR2 signaling. *FASEB J* **29**:3411-3425 https://doi.org/10.1096/fj.15-270223

32. **Casie Chetty S.,** Rost M.S., Enriquez J.R., Schumacher J.A., Baltrunaite K., Rossi A., Stainier D.Y., Sumanas S. (2017) Vegf signaling promotes vascular endothelial differentiation by modulating etv2 expression. *Dev Biol* **424**:147-161 https://doi.org/10.1016/j.ydbio.2017.03.005

33. **Perens E.A.,** Yelon D (2025) Drivers of vessel progenitor fate define intermediate mesoderm dimensions by inhibiting kidney progenitor specification. *Dev Biol* **517**:126-139 https://doi.org/10.1016/j.ydbio.2024.09.008

34. **Proulx K.,** Lu A., Sumanas S (2010) Cranial vasculature in zebrafish forms by angioblast cluster-derived angiogenesis. *Dev Biol* **348**:34-46 https://doi.org/10.1016/j.ydbio.2010.08.036

35. **Lawson N.D.,** Weinstein B.M (2002) In vivo imaging of embryonic vascular development using transgenic zebrafish. *Dev Biol* **248**:307-318 https://doi.org/10.1006/dbio.2002.0711

36. **Chestnut B.,** Sumanas S (2020) Zebrafish etv2 knock-in line labels vascular endothelial and blood progenitor cells. *Dev Dyn* **249**:245-261 https://doi.org/10.1002/dvdy.130

37. **Bertrand J.Y.,** Chi N.C., Santoso B., Teng S., Stainier D.Y., Traver D (2010) Haematopoietic stem cells derive directly from aortic endothelium during development. *Nature* **464**:108-111 https://doi.org/10.1038/nature08738

38. **Dunworth W.P.,** Cardona-Costa J., Bozkulak E.C., Kim J.D., Meadows S., Fischer J.C., Wang Y., Cleaver O., Qyang Y., Ober E.A., *et al.* (2014) Bone morphogenetic protein 2 signaling negatively modulates lymphatic development in vertebrate embryos. *Circ Res* **114**:56-66 https://doi.org/10.1161/CIRCRESAHA.114.302452

39. **Okuda K.S.,** Astin J.W., Misa J.P., Flores M.V., Crosier K.E., Crosier P.S (2012) lyve1 expression reveals novel lymphatic vessels and new mechanisms for lymphatic vessel development in zebrafish. *Development* **139**:2381-2391 https://doi.org/10.1242/dev.077701

40. **Asakawa K.,** Suster M.L., Mizusawa K., Nagayoshi S., Kotani T., Urasaki A., Kishimoto Y., Hibi M., Kawakami K (2008) Genetic dissection of neural circuits by Tol2 transposon-mediated Gal4 gene and enhancer trapping in zebrafish. *Proc Natl Acad Sci U S A* **105**:1255-1260 https://doi.org/10.1073/pnas.0704963105

41. **Grzegorski S.J.,** Chiari E.F., Robbins A., Kish P.E., Kahana A (2014) Natural variability of Kozak sequences correlates with function in a zebrafish model. *PLoS One* **9**:e108475 https://doi.org/10.1371/journal.pone.0108475

42. **Diez M.,** Medina-Munoz S.G., Castellano L.A., da Silva Pescador G., Wu Q., Bazzini A.A. (2022) iCodon customizes gene expression based on the codon composition. *Sci Rep* **12**:12126 https://doi.org/10.1038/s41598-022-15526-7

43. **Villefranc J.A.,** Amigo J., Lawson N.D (2007) Gateway compatible vectors for analysis of gene function in the zebrafish. *Dev Dyn* **236**:3077-3087 https://doi.org/10.1002/dvdy.21354

44. **Choi H.M.T.,** Schwarzkopf M., Fornace M.E., Acharya A., Artavanis G., Stegmaier J., Cunha A., Pierce N.A (2018) Third-generation in situ hybridization chain reaction: multiplexed, quantitative, sensitive, versatile, robust. *Development* **145** https://doi.org/10.1242/dev.165753

45. **Jowett T** (1999) Analysis of protein and gene expression. *Methods Cell Biol* **59**:63-85 https://doi.org/10.1016/s0091-679x(08)61821-x

46. **Reischauer S.,** Stone O.A., Villasenor A., Chi N., Jin S.W., Martin M., Lee M.T., Fukuda N., Marass M., Witty A., *et al.* (2016) Cloche is a bHLH-PAS transcription factor that drives haemato-vascular specification. *Nature* **535**:294-298 https://doi.org/10.1038/nature18614

47. **Sumanas S.,** Jorniak T., Lin S (2005) Identification of novel vascular endothelial-specific genes by the microarray analysis of the zebrafish cloche mutants. *Blood* **106**:534-541 https://doi.org/10.1182/blood-2004-12-4653

48. **Liao E.C.,** Paw B.H., Oates A.C., Pratt S.J., Postlethwait J.H., Zon L.I (1998) SCL/Tal-1 transcription factor acts downstream of cloche to specify hematopoietic and vascular progenitors in zebrafish. *Genes Dev* **12**:621-626 https://doi.org/10.1101/gad.12.5.621

49. **Potter A.S.,** Steven Potter S (2019) Dissociation of Tissues for Single-Cell Analysis. *Methods Mol Biol* **1926**:55-62 https://doi.org/10.1007/978-1-4939-9021-4_5

50. **Hao Y.,** Hao S., Andersen-Nissen E., Mauck W.M., Zheng S., Butler A., Lee M.J., Wilk A.J., Darby C., Zager M., *et al.* (2021) Integrated analysis of multimodal single-cell data. *Cell* **184**:3573-3587.e3529. https://doi.org/10.1016/j.cell.2021.04.048

51. **Wickham H.** (2016) *ggplot2 : Elegant Graphics for Data Analysis* (2nd ed) Springer International Publishing.

52. **Wickham H A.M.,** Bryan J, Chang W, McGowan LD, François R, Grolemund G, Hayes A, Henry L, Hester J, Kuhn M, *et al.* (2019) Welcome to the tidyverse. *Journal of Open Source Software* https://doi.org/10.21105/joss.01686

53. **Wickham H** (2007) Reshaping Data with the reshape Package. *Journal of Statistical Software* **21**:1-20

54. **Wickham H F.R.,** Henry L, Müller K, Vaughan D (2023) dplyr: A Grammar of Data Manipulation.

55. **Hao Y.,** Stuart T., Kowalski M.H., Choudhary S., Hoffman P., Hartman A., Srivastava A., Molla G., Madad S., Fernandez-Granda C., *et al.* (2024) Dictionary learning for integrative, multimodal and scalable single-cell analysis. *Nat Biotechnol* **42**:293-304 https://doi.org/10.1038/s41587-023-01767-y

56. **R Core Team** (2025) R: A language and environment for statistical computing.

57. **Rstudio Team** (2020) RStudio: Integrated Development for R (RStudio, Inc.).

Gurung S, Metikala S, Sumanas S (2021) Single-cell transcriptomic analysis of 36 hpf Zebrafish etv2 and jam2b positive cells. NCBI Gene Expression Omnibus. ID GSE179926 https://www.ncbi.nlm.nih.gov/geo/query/acc.cgi?acc=GSE179926

Peer reviews

Reviewer #1 (Public review):

The manuscript by Griciunaite et al. explores jam2b functions in the formation of late vascular precursors in what is termed the secondary heart field. The authors nicely show that expression of jam2b defines these cells in the lateral plate mesoderm and the intestinal vasculature using a target integration of Gal4 into the jam2b locus. This analysis is followed by using a UAS:cre approach to follow the lineage of jam2b expressing cells, demonstrating their contributions to the vasculature during a second round of specification of vascular precursors. This is confirmed with single-cell analysis of jam2b-gal4 expressing cells. The authors then explore the genetic requirements of jam2a and b in zebrafish and also show that hand2 functions in the secondary heart field upstream of jam2b.

Overall, the experimental evidence and results support the major conclusions. The study elucidates a novel role for jam2 in the specification of vascular precursors at later stages of development.

This understanding has important implications for treating vascular disease and regenerative therapies. The manuscript is very clearly written, and the major conclusions are likely to have a lasting impact on the field.

https://doi.org/10.7554/eLife.109406.1.sa2

Reviewer #2 (Public review):

Summary:

Griciunaite et al. report on the function of jam2b and hand2 in the formation of the intestinal vasculature derived from late-forming endothelial cells (ECs) within the secondary vascular field (SVF). They generate transgenic lines that allow for the tracking of jam2b-expressing cells, both with fluorescent proteins and through Cre-mediated recombination in reporter lines. They also show that double maternal zygotic mutants in jam2a and jam2b, as well as hand2 mutants, display defects in the formation of the intestinal vasculature.

Strengths:

The results are interesting, as they address the important question of how blood vessels form during later developmental time points and potentially identify specific genes regulating this process.

Weaknesses:

(1) The authors generate a new tool, a Gal4 knock-in of the jam2b locus, to track EGFP-expressing cells over time and follow the developmental trajectory of jam2b-expressing cells. Figure 1 characterizes the line. However, it lacks quantification, e.g., how many etv2-expressing cells also show EGFP expression or the contribution of EGFP-expressing cells to different types of blood vessels. This type of quantification would be useful, as it would also allow for comparison of their findings to their previous data examining the contribution of SVF cells to different types of blood vessels. All the authors state that at 30 hpf, EGFP-expressing cells can be seen in the vasculature (apparently the PCV).

It is not clear why the authors do not use a nuclear marker for both ECs (as they did in their previous publication) and for jam2b-expressing cells. UAS:nEGFP and UAS:NLS-mcherry (e.g. pt424tg) transgenic lines are available. This would circumvent the problem the authors

encounter with the strong fluorescence visible in the yolk extension. It would also facilitate quantifying the contribution of jam2b cells to different types of blood vessels.

(2) The time-lapse movie in Figure 2 is not very informative, as it just provides a single example of a dividing cell contributing to the PCV. Also, quantifications are needed. As SVF cells appear to expand significantly after their initial specification, it would be informative to know how many cell divisions and which types of blood vessels jam2b-expressing cells contribute to. Can the authors observe cells that give rise to different types of blood vessels? Jam2b expression in LPM cells apparently precedes expression of etv2. Is etv2 needed for maintenance, or do Jam2b-expressing cells contribute to different types of tissues in etv2 mutant embryos? Comparing time-lapse analysis in wildtype and etv2 mutant embryos would address this question.

(3) In Figure 3, the authors generate UAS:Cre and UAS:Cre-ERT2 transgenic lines to lineage trace the jam2b-expressing cells. It is again not clear why the authors do not use a responder line containing nuclear-localized fluorescent proteins to circumvent the strong expression of fluorescent proteins in the yolk extension. It is also unclear why the two transgenic lines give very different results regarding the number of cells being labelled. The ERT2 fusions label around 3 cells in the SIA, while the Cre line labels only about 1.5 cells per embryo, with very little contribution of labelled cells to other blood vessels. One would expect the Cre line requiring tamoxifen induction to label fewer cells when compared to the constitutive Cre line. What is the reason for this discrepancy? Are the lines single integration? Is there silencing? This needs to be better characterized, also regarding the reproducibility of the experiments. If the Cre lines were to be multiple copy integrations, outcrossing the line might lead to lower expression levels in future generations.

It is also not clear how the authors conclude from these findings that "SVF cells show major contribution to the SIA and SIV" when only 1.5 or 3 cells of the SIA are labelled, with even fewer cells labelled in other blood vessels. They speculate that this might be due to low recombination efficiency, a question they then set out to answer using photoconversion of etv2:KAEDE expressing cells, an experiment that they also performed in their 2014 and 2022 publications. To check for low recombination efficiency, the authors could examine the expression of Cre mRNA in their transgenic embryos. Do many more jam2b expressing cells express Cre mRNA than they observe in their switch lines? They could also compare their experiments using Cre recombinase with those using EGFP expression in jam2b cells. EGFP is relatively stable, and the time frames the authors analyze are short. As no quantification of EGFP-expressing cells is provided in Figure 1, this comparison is currently not possible. Do these two different approaches answer different questions here?

(4) Concerning the etv2:KAEDE photoconversion experiments: The percentages the authors report for SVF cells' contribution to the SIV and SIA differ from their previous study (Dev Cell, 2022). In that publication, SVF cells contributed 28% to the SIA and 48% to the SIV. In the present study, the numbers are close to 80% for both vessels. The difference is that the previous study analyzed 2dpf old embryos and the new one 4dpf old embryos. Do SVF-derived cells proliferate more than PCV-derived cells, or is there another explanation for this change in percentage contribution?

(5) Single-cell sequencing data: Why do the authors not show jam2b expression in their single-cell sequencing data? They sorted for (presumably) jam2b-expressing cells and hypothesize that jam2b expression in ECs at this time point is important for the generation of intestinal vasculature. Do ECs in cluster 15 express jam2b? Why are no other top marker genes (tal1, etv2, egfl7, npas4l) included in the dot blot in Figure 5b?

(6) Concerns about cell autonomy of mutant phenotypes: The authors need to perform in situ hybridization to characterize jam2a expression. Can it be seen in SVF cells? The double mutants show a clear phenotype in intestinal vessel development; however, it is unclear

whether this is due to a cell-autonomous function of jam2a/b within SVF cells. The authors need to address this issue, as jam2b and potentially also jam2a are expressed within the tissue surrounding the forming SVF. For instance, do transplanted mutant cells contribute to the intestinal vasculature to the same extent as wild-type cells do?

(7) Finally, the authors analyze the phenotypes of hand2 mutants and their impact on the expression of jam2b and etv2. They observe a reduction in jam2b and etv2 expression in SVF cells. However, they do not show the vascular phenotypes of hand2 mutants. Is the formation of the SIA and SIV disturbed? Is hand2 cell autonomously needed in ECs? The authors suggest that hand2 controls SVF development through the regulation of jam2b. However, they also show that jam2b mutants do not have a phenotype on their own. Clearly, hand2, if it were to be required in ECs, regulates other genes important for SVF development. These might then regulate jam2b expression. The clear linear relationship, as the title suggests, is not convincingly shown by the data.

https://doi.org/10.7554/eLife.109406.1.sa1

Reviewer #3 (Public review):

Summary:

This study by Griciunaite et al. investigates the function of the adhesion molecule Jam2 in initiating the formation of organ (intestinal)-specific vasculature in zebrafish. Their previous studies identified a group of late-forming vascular progenitors from the lateral plate mesoderm along the yolk extension termed the secondary vascular field (SVF), which can contribute to intestinal vasculature. Transcriptomic analysis of the zebrafish trunk region identified SVF-enriched marker genes, which include jam2b. They then performed expression analysis of jam2b using whole-mount in situ hybridization and Gal4 knock-in transgenic line analysis. These analyses show that jam2b is expressed in the SVF cells that correspond to etv2 and kdrl expression past 24 hours. Lineage tracing combining jam2b:Gal4 and UAS:Cre or UAS:CreERT2 show the contribution of jam2b in SVF and intestinal vasculature formation. jam2b mutations did not cause observable defects in the vasculature, but combined jam2a; jam2b mutations led to impaired ISV, PCV, SIA, SIV and thoracic duct lymphatic vasculature formation. Finally, the authors show that mutations in the transcription factor hand2 led to reduced jam2b expression and impaired SVF formation.

Strengths:

The authors accomplished many feats in generating new reporter lines and mutations that are valuable to the community. The study provided an interesting perspective on organ-specific vascular development and origin heterogeneity. The genetic aspects of the study are clean, and the mutational phenotypes are convincing.

Several suggestions and major comments that can improve the manuscript include:

(1) Overall molecular mechanisms of Jam2 function are not fully uncovered in the study. How do the adhesion molecules Jam2a and Jam2b regulate SVF cell formation? Are they responsible for migration, adhesion or fate determination of these structures? The authors should provide a more in-depth study of the jam2a, jam2b mutations and assess the processes affected in these mutants. Combining these mutants with etv2:Kaede can also provide a stronger causative link between their functions and defects in SVF formation.

(2) Have the authors tested the specificity of the jam2b knock-in reporter line? This is an important experiment, as many of the conclusions derive from lineage tracing and fluorescence reporting from this knock-in line. One suggestion is to cross the jam2b:GFP or jam2b:Gal4, UAS:GFP line to the generated jam2b mutants, and examine the expression

pattern of these lines. Considering that the ISH experiment showed lack of jam2b expression, the reporter line should not be expressed in the jam2b mutants.

(3) The rationale behind the regeneration study is not clear, and the mechanisms underlying the phenotype are not well described. How do the authors explain the phenotype with the impaired regeneration, and what is the significance of this finding as it relates to SVF formation and function?

(4) The authors need to include representative images of jam2b>CreERT2 with 4-OH activation at different timepoints in Figure 3.

(5) The etv2:Kaede photoconversion experiment to show that the majority of intestinal vasculature derives after 24 hours needs to be supplemented with additional data on photoconverted post-24-hour-old endothelial cells, with the expectation that the majority of intestinal endothelial cells at 4 days will then be labeled with red Kaede. In addition, there have been data that show the red Kaede protein is not stable past several days in vivo, and 3 days might be sufficient for the removal or degradation of this photoconverted protein. Thus, the statement that intestinal vasculature forms largely by new vasculogenesis might be too strong based on existing data.

(6) To strengthen the claim that hand2 acts upstream of jam2b, the authors can perform combinatorial genetic epistatic analysis and examine whether jam2b mutations worsen hand2 homozygous or heterozygous effects on the SVF. Similarly, overexpressing jam2b might rescue the loss of SVF/etv2 expression in hand2 mutants.

https://doi.org/10.7554/eLife.109406.1.sa0

Author response:

We thank all reviewers for their comments. We appreciate the acknowledgement that the paper is important and that results support the major conclusions. We are planning to address the specific concerns as noted by the reviewers in the following way:

> ***Public Reviews:***
>
> ***Reviewer #2 (Public review):***
>
> *(1) The authors generate a new tool, a Gal4 knock-in of the jam2b locus, to track EGFP-expressing cells over time and follow the developmental trajectory of jam2b-expressing cells. Figure 1 characterizes the line. However, it lacks quantification, e.g., how many etv2-expressing cells also show EGFP expression or the contribution of EGFP-expressing cells to different types of blood vessels. This type of quantification would be useful, as it would also allow for comparison of their findings to their previous data examining the contribution of SVF cells to different types of blood vessels. All the authors state that at 30 hpf, EGFP-expressing cells can be seen in the vasculature (apparently the PCV).*
>
> *It is not clear why the authors do not use a nuclear marker for both ECs (as they did in their previous publication) and for jam2b-expressing cells. UAS:nEGFP and UAS:NLS-mcherry (e.g. pt424tg) transgenic lines are available. This would circumvent the problem the authors encounter with the strong fluorescence visible in the yolk extension. It would also facilitate quantifying the contribution of jam2b cells to different types of blood vessels.*

We agree with the importance of quantification. We had performed quantification of *jam2b*$^{Gt(2A\text{-}Gal4)}$*;UAS:GFP* contribution to different vascular beds, which was shown in Suppl. Fig. S3. We will clarify this in the revision. We also agree that nuclear GFP or mCherry would help to visualize and quantify cells. Unfortunately, we do not have nuclear UAS:GFP or

UAS:mCherry line in our possession, and it will take too long to import it for the standard revision timeline. We are working on the construct, and will attempt to establish the line; therefore we are hoping to clarify these results with the nuclear line in the revised manuscript.

> *(2) The time-lapse movie in Figure 2 is not very informative, as it just provides a single example of a dividing cell contributing to the PCV. Also, quantifications are needed. As SVF cells appear to expand significantly after their initial specification, it would be informative to know how many cell divisions and which types of blood vessels jam2b-expressing cells contribute to. Can the authors observe cells that give rise to different types of blood vessels? Jam2b expression in LPM cells apparently precedes expression of etv2. Is etv2 needed for maintenance, or do Jam2b-expressing cells contribute to different types of tissues in etv2 mutant embryos? Comparing time-lapse analysis in wildtype and etv2 mutant embryos would address this question.*

The time-lapse was meant to serve as an illustration and confirmation of *jam2b* cell contribution to vasculature. As noted above, Suppl. Fig. S3 provides quantification of *jam2b* cell contribution to different vascular beds. We had previously performed detailed time-lapse analysis and quantification of SVF cell migration to PCV, SIA and SIV using *etv2-2A-Venus* line (Metikala et al 2022, Dev Cell), which has some of the same (or similar) information. It is very challenging to obtain this data using *jam2b* reporter line due to extensive and bright GFP expression in the mesothelial layer over the yolk and yolk extension; for that reason we can only trace some GFP cells but not all of them. Regarding *etv2* requirement for *jam2b* maintenance, we intend to address this question by analyzing *jam2b* cell contribution in *etv2* MO injected embryos, which recapitulates the phenotype in *jam2b* mutants.

> *(3) In Figure 3, the authors generate UAS:Cre and UAS:Cre-ERT2 transgenic lines to lineage trace the jam2b-expressing cells. It is again not clear why the authors do not use a responder line containing nuclear-localized fluorescent proteins to circumvent the strong expression of fluorescent proteins in the yolk extension. It is also unclear why the two transgenic lines give very different results regarding the number of cells being labelled. The ERT2 fusions label around 3 cells in the SIA, while the Cre line labels only about 1.5 cells per embryo, with very little contribution of labelled cells to other blood vessels. One would expect the Cre line requiring tamoxifen induction to label fewer cells when compared to the constitutive Cre line. What is the reason for this discrepancy? Are the lines single integration? Is there silencing? This needs to be better characterized, also regarding the reproducibility of the experiments. If the Cre lines were to be multiple copy integrations, outcrossing the line might lead to lower expression levels in future generations.*
>
> *It is also not clear how the authors conclude from these findings that "SVF cells show major contribution to the SIA and SIV" when only 1.5 or 3 cells of the SIA are labelled, with even fewer cells labelled in other blood vessels. They speculate that this might be due to low recombination efficiency, a question they then set out to answer using photoconversion of etv2:KAEDE expressing cells, an experiment that they also performed in their 2014 and 2022 publications. To check for low recombination efficiency, the authors could examine the expression of Cre mRNA in their transgenic embryos. Do many more jam2b expressing cells express Cre mRNA than they observe in their switch lines? They could also compare their experiments using Cre recombinase with those using EGFP expression in jam2b cells. EGFP is relatively stable, and the time frames the authors analyze are short. As no quantification of EGFP-expressing cells is provided in Figure 1, this comparison is currently not possible. Do these two different approaches answer different questions here?*

The reviewer brings up important points, we appreciate that. Unfortunately, we do not have a nuclear switch line in our possession, and it is not possible to obtain it in the normal

manuscript revision time line. Regarding UAS:Cre and UAS:CreERT2 lines, they both show rather similar labeling, with most labeled cells present in the SIA. The difference in cell number (1.5 versus 3) is likely due to different levels of Cre expression, which may vary dependent on the integration site. The lines most likely are multi-copy integrations, which can be helpful, as this would result in higher Cre expression. We will address the silencing question by performing in situ hybridization or HCR analysis for Cre or CreERT2 and comparing it with endogenous *jam2b* expression, as the reviewer suggested. We have noticed that the switch line used, *actb2:loxP-BFP-loxP-dsRed*, exhibits lower recombination frequency compared to other switch lines (we used it because it was compatible with endothelial fli1:GFP line). We will attempt to answer this question by crossing to other switch lines, which may exhibit higher recombination frequency. In principle, UAS:GFP and switch lines should produce a similar result, except that GFP decays over time and therefore our initial expectation was that switch lines may produce a more accurate result. However, this may not be the case due to low recombination efficiency, which we will attempt to address in the revision.

> *(4) Concerning the etv2:KAEDE photoconversion experiments: The percentages the authors report for SVF cells' contribution to the SIV and SIA differ from their previous study (Dev Cell, 2022). In that publication, SVF cells contributed 28% to the SIA and 48% to the SIV. In the present study, the numbers are close to 80% for both vessels. The difference is that the previous study analyzed 2dpf old embryos and the new one 4dpf old embryos. Do SVF-derived cells proliferate more than PCV-derived cells, or is there another explanation for this change in percentage contribution?*

These numbers refer to different experiments; we apologize for the confusion. As reported earlier in Metikala et 2022, 28% of SVF cells contributed to the SIA and 48% to the SIV by 3 dpf (not 2 dpf; only PCV analysis was done at 2 dpf); SIA and SIV analysis was done based on time-lapse image analysis of etv2-2A-Venus line at 3 dpf, shown in Fig. 3C in Metikala et al. However, this only refers to SVF cell contribution. It does not mean that 28% or 48% cells in SIA or SIV are derived from SVF. The total fraction of SIA and SIV cells that are derived from SVF has not been quantified in the previous study, because that would require accurate tracking of all SVF cells, which is experimentally challenging. Etv2:Kaede experiment is slighly different, because it reports newly formed cells after 24 hpf. It cannot tell if new cells are all derived from SVF cells, although we are not aware of any other source of new endothelial cells at these stages. In the previous study by Metikala et al 2022, we reported ~22 newly formed SIA and ~50 newly formed cells in SIV by 3 dpf (Fig. 1 in Metikala et al 2022), although the entire number of cells was not quantified, therefore the percentage was not known. In the current study, we attempted to estimate the entire percentage of green only Kaede cells, which was close to 80% in both SIA or SIV at 4 dpf. Please note that this estimate was performed in the posterior portion of SIA and SIV that overlies the yolk extension and where SVF cells are observed. We did not quantify cells in the anterior SIV portion, which forms the basket over the yolk.

> *(5) Single-cell sequencing data: Why do the authors not show jam2b expression in their single-cell sequencing data? They sorted for (presumably) jam2b-expressing cells and hypothesize that jam2b expression in ECs at this time point is important for the generation of intestinal vasculature. Do ECs in cluster 15 express jam2b? Why are no other top marker genes (tal1, etv2, egfl7, npas4l) included in the dot blot in Figure 5b?*

We appreciate the suggestion and will include additional marker genes as well as *jam2b* in the revised version of the manuscript.

> *(6) Concerns about cell autonomy of mutant phenotypes: The authors need to perform in situ hybridization to characterize jam2a expression. Can it be seen in SVF cells? The double mutants show a clear phenotype in intestinal vessel development; however, it is unclear whether this is due to a cell-autonomous function of jam2a/b within SVF cells.*

> *The authors need to address this issue, as jam2b and potentially also jam2a are expressed within the tissue surrounding the forming SVF. For instance, do transplanted mutant cells contribute to the intestinal vasculature to the same extent as wild-type cells do?*

jam2a expression has been characterized in the previous studies and it is shown in the Suppl. Fig. S4E. It is primarily enriched in the skeletal muscle. However, our single-cell RNA-seq analysis shows that SVF cells also express *jam2a*. We will include additional data on *jam2a* expression in the revised manuscript. We agree that transplation to address cell autonomy is an important experiment, yet there are some practical challenges to it. *Jam2a,jam2b* mutant phenotype is only partially penetrant, and about 50% reduction in SVF cell number, as well as partial SIA and SIV phenotypes are observed. Only a small number of transplanted cells may contribute to intestinal vasculature, therefore it may be challenging to see the differences, given the partial penetrance. In an attempt to address cell -autonomy question, we will try a different approach. We will overexpress *jam2b* labeled with 2A-mCherry, and test if it can rescue the mutant phenotype in cell autonomous manner. Overexpression will be done in a mosaic manner, with higher number of cells labeled than in a typical transplantation experiment.

> *(7) Finally, the authors analyze the phenotypes of hand2 mutants and their impact on the expression of jam2b and etv2. They observe a reduction in jam2b and etv2 expression in SVF cells. However, they do not show the vascular phenotypes of hand2 mutants. Is the formation of the SIA and SIV disturbed? Is hand2 cell autonomously needed in ECs? The authors suggest that hand2 controls SVF development through the regulation of jam2b. However, they also show that jam2b mutants do not have a phenotype on their own. Clearly, hand2, if it were to be required in ECs, regulates other genes important for SVF development. These might then regulate jam2b expression. The clear linear relationship, as the title suggests, is not convincingly shown by the data.*

As suggested, we will add the analysis of SIA and SIV in *hand2* mutants during the revision process. We could not assess that easily because the line was not maintained in vascular *fli1:GFP* background. We do not know if *hand2* is required cell-autonomously. This is an important question, but it may be answered better in a separate study. Regarding *hand2-jam2b* axis, it is very clear that *jam2b* expression in the posterior lateral plate mesoderm is completely lost in *hand2* mutants, except for its more anterior domain over the yolk. This does support the idea that *hand2* functions upstream of *jam2b*. However, the relationship may not be necessarily direct. We agree that *hand2* may regulate additional genes involved in SVF cell development. We will attempt to clarify this relationship and test if *jam2b* overexpression may rescue *hand2* mutant phenotype.

> ***Reviewer #3 (Public review):***
>
> *(1) Overall molecular mechanisms of Jam2 function are not fully uncovered in the study. How do the adhesion molecules Jam2a and Jam2b regulate SVF cell formation? Are they responsible for migration, adhesion or fate determination of these structures? The authors should provide a more in-depth study of the jam2a, jam2b mutations and assess the processes affected in these mutants. Combining these mutants with etv2:Kaede can also provide a stronger causative link between their functions and defects in SVF formation.*

Our data argue that the initial SVF cell specification (based on *etv2* expression) is reduced in *jam2a;jam2b* mutants. We do not know if the migration or fate determination of the remaining SVF cells is also affected, although this may be more challenging to answer, as there are only few SVF cells remaining. We agree that further mechanistic studies of *jam2a,jam2b* function are needed. However, we think that this would be better addressed in a separate study. We are currently raising mutants crossed into *fli1:Kaede* line, which should

confirm that there are fewer new cells that emerge after Kaede photoconversion in *jam2a,jam2b* mutants.

> *(2) Have the authors tested the specificity of the jam2b knock-in reporter line? This is an important experiment, as many of the conclusions derive from lineage tracing and fluorescence reporting from this knock-in line. One suggestion is to cross the jam2b:GFP or jam2b:Gal4, UAS:GFP line to the generated jam2b mutants, and examine the expression pattern of these lines. Considering that the ISH experiment showed lack of jam2b expression, the reporter line should not be expressed in the jam2b mutants.*

We show in Suppl. Fig. 2 that *jam2b*$^{Gt(2A\text{-}Gal4)}$*;UAS:GFP* knock-in line has similar expression pattern as *jam2b* mRNA by in situ hybridization, which argues for its specificity. In the revision, we plan to use HCR analysis to confirm than *jam2b* mRNA is expressed in the same cells as *jam2b*$^{Gt(2A\text{-}Gal4)}$*;UAS:GFP*, as an additional evidence for its specificity. Unfortunately, it is not feasible to cross *jam2b* knock-in line into *jam2b* mutants, as suggested by the reviewer. Because *jam2b* knock-in line targets the endogenous *jam2b* genomic locus, which is very close in the genome to *jam2b* promoter deletion in *jam2b* mutants, the recombination frequency would be very low, and we would not get double *jam2b* knock-in and knock-out events in the same chromosome.

> *(3) The rationale behind the regeneration study is not clear, and the mechanisms underlying the phenotype are not well described. How do the authors explain the phenotype with the impaired regeneration, and what is the significance of this finding as it relates to SVF formation and function?*

We apologize for this omission. This experiment was more thouroughly described in our previous study by Metikala et al 2022. In that study we showed that when endothelial cells are ablated by treating with MTZ from 6 to 45 hpf, this results in ablation of all vascular endothelial cells except for SVF cells, because they originate later than other cells. We subsequently showed that these SVF cells can partially form PCV and intestinal vasculature, helping them regenerate, which was confirmed by time-lapse imaging. In the current study, we tested if *jam2a; jam2b* double mutants show defects in such vascular regeneration. Indeed, regeneration after cell ablation was reduced, which correlated with reduction in SVF cell number. This argues that jam2a/b function is required for SVF cell emergence and vascular recovery after endothelial cell ablation. We will provide better description of this experiment and discuss interpretations in the revised manuscript.

> *(4) The authors need to include representative images of jam2b>CreERT2 with 4-OH activation at different timepoints in Figure 3.*

Yes, thanks for noting this; these images will be included in the revised manuscript.

> *(5) The etv2:Kaede photoconversion experiment to show that the majority of intestinal vasculature derives after 24 hours needs to be supplemented with additional data on photoconverted post-24-hour-old endothelial cells, with the expectation that the majority of intestinal endothelial cells at 4 days will then be labeled with red Kaede. In addition, there have been data that show the red Kaede protein is not stable past several days in vivo, and 3 days might be sufficient for the removal or degradation of this photoconverted protein. Thus, the statement that intestinal vasculature forms largely by new vasculogenesis might be too strong based on existing data.*

It is apparent from Fig. 4B that many other vessels, such as the dorsal aorta and many intersegmental vessels show robust red Kaede expression at 4 dpf, arguing that there is sufficient photoconverted Kaede present at this stage, and its degradation is unlikely to be the reason. However, we are planning to include additional control experiments, as suggested by the reviewer, to make this argument stronger.

> *(6) To strengthen the claim that hand2 acts upstream of jam2b, the authors can perform combinatorial genetic epistatic analysis and examine whether jam2b mutations worsen hand2 homozygous or heterozygous effects on the SVF. Similarly, overexpressing jam2b might rescue the loss of SVF/etv2 expression in hand2 mutants.*

We appreciate this suggestion. Double epistatic analysis, while informative, can be tricky. In this case, we are dealing with *jam2a; jam2b* redundancy and also the maternal effect. It may take a while considerable effort to generate different combinations of tripple mutant lines (jam2a,jam2b,hand2), and it is unclear whether double or tripple heterozygous embryos will show any defects to clarify their epistatic relationship. Instead, as suggested, we are planning to overexpress *jam2b* in wild-type and *hand2* mutants to address this point.

https://doi.org/10.7554/eLife.109406.1.sa4